DETERMINATION OF SUB-CELLULAR LOCALIZATION OF POTATO VIRUS X REPLICASE DURING INFECTION

By

DEVINKA C. N. BAMUNUSINGHE

Bachelor of Science

University of Ruhuna

Sri Lanka

2002

Submitted to the Faculty of the
Graduate College of the
Oklahoma State University
in partial fulfillment of
the requirements for
the Degree of
MASTER OF SCIENCE
May, 2008

DETERMINATION OF SUB-CELLULAR LOCALIZATION OF POTATO VIRUS X REPLICASE DURING INFECTION

Thesis Approved:

Dr. Jeanmarie Verchot–Lubicz

Thesis Adviser

Dr. Nathan Walker

Committee Member

Dr. Richard S. Nelson

Committee Member

Dr. A. Gordon Emslie

Dean of the Graduate College

ACKNOWLEDGEMENTS

It is with great pleasure, that I express my deep appreciation to my supervisor Dr. Jeanmarie Verchot-Lubicz, Department of Entomology and Plant Pathology, Oklahoma State University for valuable guidance and insight throughout the research. I wish to mention with deep gratitude about her constructive advice given, which induced me to further my knowledge and solve the research problems. I take this opportunity to thank Dr. Ulrich Melcher, Department of Biochemistry and Molecular Biology, Oklahoma State University, NSF and EPSCOR projects for funding me through out my research. Special vote of thanks goes to my Committee members, Dr. Nathan Walker, Department of Entomology and Plant Pathology, Oklahoma State University and Dr. Richard S. Nelson, Noble Foundation, Ardmore, OK for their valuable suggestions and comments. I also like to thank Dr. Jian-Zhong Liu from Noble Foundation, Ardmore, OK for teaching me immunolabeling techniques and Dr. Richard S. Nelson for making it possible and providing his lab and resources. The technical assistance and sample preparation for transmission electron microscopy and confocal microscopy throughout my research by Dr. Charlotte Ownby, Terry Colberg and Dr. Susheng Tan from OSU Electron and Confocal Microscopy Center are gratefully acknowledged. I also like to thanks Dr. Ben Fowler and Joe Wilkerson from OKC medical research institute for sample preparation for transmission electron microscopy. I also like to thank Dr. Udaya De Silva for introducing me to my adviser. I express my thanks and appreciation to my mom Mrs. Sita Bamunusinghe, my two sisters and brother for their love, motivation and encouragements and my dad Late Mr. Chandrasiri Bamunusinghe for his affection. Lastly, but in no sense the least, I am thankful to all my friends who made my stay at the university a memorable and valuable experience, my lab members Dr. Ho-Jong Ju, Dr. Chang Ming Ye, Dr. Tefera Mekuria, Dr. Tim Samuel and James Brown for their friendship and support, academic staff for broadening my knowledge and non-academic staff, Lisa and Janet in co-facility for their support in numerous ways.

TABLE OF CONTENTS

LIST OF TABLES

Tables Page

CHAPTER IV

LIST OF FIGURES

CHAPTER I

INTRODUCTION AND OBJECTIVES

Introduction

Potato virus X (PVX) encodes a single 166 kDa protein that is the viral replicase. This protein contains methyltransferase, helicase, and polymerase domains. Since replication of positive strand RNA viruses is typically membrane-associated, my objective is to determine if the PVX replicase associates with cellular membranes during infection. Immunofluorescence labeling will be used to determine where the PVX replicase accumulates in PVX-infected tobacco protoplast and leaves. Infection foci from inoculated leaves will be cryo-fixed and embedded in LR-White. Immunogold labeling of thin sections will be conducted to study the membrane association of the viral replicase.

Since the PVX triple gene block protein 2 (TGBp2) and TGBp3 are also membrane-associated proteins, experiments will be conducted to determine if these proteins co-localize with the PVX replicase during infection. The PVX.GFP-TGBp2 and PVX-TGBp3-GFP infectious clones will be used to study co-localization of TGBp2 and TGBp3 with the viral replicase (Fig 1). The GFP-TGBp2 fusion contains GFP fused to the 5' end of the TGBp2 coding sequence. The TGBp3-GFP fusion contains GFP fused to the 3' end of the PVX TGBp3 coding sequence. These fusions were introduced into the

PVX genome and GFP is used to track the sub-cellular distribution of TGBp2 and TGBp3 respectively during virus infection. Immunofluorescence and immunogold labeling of infected tobacco protoplasts and plants will be used to determine if TGBp2 and TGBp3 co-localize with the PVX replicase during virus infection. Evidence that TGBp2 or TGBp3 co-localize with the replicase would suggest that these proteins interact to promote virus infection.

Objectives

1) Determine the sub-cellular localization of the PVX replicase during infection in protoplasts. Determine if TGBp2 and TGBp3 co-localize with the PVX replicase.

2) Determine the sub-cellular localization of the PVX replicase during infection in plants. Determine if TGBp2 and TGBp3 co-localize with the PVX replicase.

3) Conduct electron microscopy to determine the sub-cellular location of the PVX replicase during infection and to determine if TGBp2 and TGBp3 co-localize with the replicase in plants.

4) Conduct membrane fractionations to determine if the PVX replicase, TGBp2, and TGBp3 co-localize.

CHAPTER II

REVIEW OF LITERATURE

PVX Genome.

Potato virus X (PVX) is the type member of the *Potexvirus* genus. It is 6.4 kb (Baulcombe *et al*., 1995; Huisman *et al*., 1998), single-stranded, positive-sense RNA virus which is capped at the 5' end (Sonenberg *et al*., 1978) and polyadenylated at the 3' end. The PVX genome contains five open reading frames (ORFs) (Huisman *et al*., 1988) (Figure1). The first ORF encodes a 166 kDa replicase protein (Huisman *et al*., 1988). The replicase ORF is followed by three partially overlapping ORFs called the triple gene block (TGB) which encode three movement proteins named TGBp1, TGBp2, and TGBp3 (Beck *et al.*,1991; Verchot *et al.*, 1998). These TGB proteins are conserved in potex-, beny-, carla-, hordei- and pecluviruses (Memelink *et al*., 1990; Morozov *et al*., 1999; Morozov *et al*., 1987; Skryabin *et al*., 1988). The PVX coat protein ORF is near the 3' end of the genome (Huisman *et al.*, 1988). PVX TGBp1 is an RNA helicase and is responsible for increasing plasmodesmata permeability for virus movement (Howard *et al*., 2004; Lough *et al*., 1998; 2000; Angel *et al*., 1996). PVX TGBp2 and TGBp3 associate with endoplasmic reticulum (ER) (Krishnamurthy *et al.*, 2003; Mitra *et al.*, 2003). TGBp2 induces vesicles to bud from the ER network (Ju *et al.*, 2005). The role of the ER and of ER-derived vesicles in PVX movement is unknown.

In the 1990s infectious clones of PVX were constructed. PVX cDNAs were inserted into plasmids adjacent to the bacteriophage T7 promoter (Baulcombe *et al.*, 1995). Infectious transcripts can be synthesized *in vitro* and used to inoculate plants. The advantage of using an infectious clone rather than purified virus is ease of preparing virus, the plasmids can be maintained longer than the purified virus and we can introduce mutations into the viral genome to test gene functions. For the PVX infectious clone, the CP subgenomic promoter was duplicated and the green fluorescent protein (GFP) coding sequence was inserted into the viral genome. GFP expression is used to visual virus infection as it spreads from cell to cell and from leaf to leaf (Baulcombe *et al.*, 1995) (Fig 1a). We also deleted the TGBp2 coding sequence and introduced a GFP-TGBp2 fusion next to the duplicated coat protein subgenomic promoter. This PVX.GFP-TGBp2 is infectious and has been used to study the subcellular distribution of TGBp2 during PVX infection in protoplast and tobacco leaves (Ju *et al.*, 2005; Mitra *et al.*, 2003) (Fig 1b). The PVX.TGBp3-GFP infectious clone was recently prepared and contains the GFP coding sequence directly fused to the TGBp3 coding sequence (Fig 1c).

(a) PVX.GFP

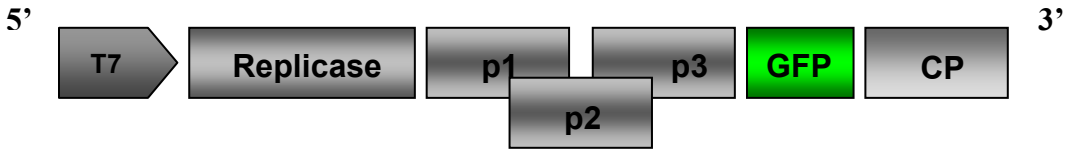

(b) PVX.GFP-TGBp2

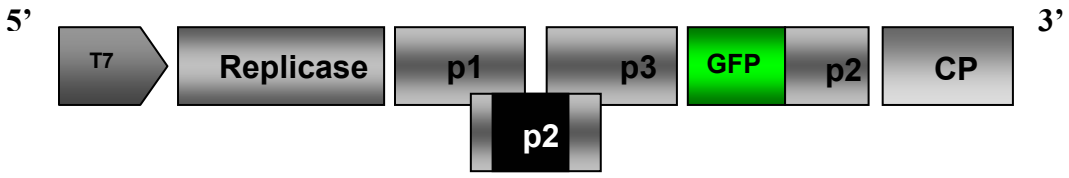

(c) PVX.TGBp3-GFP

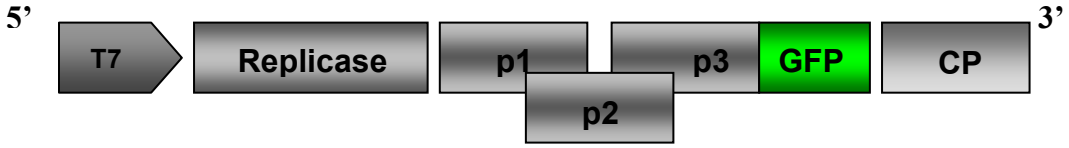

Fig 1: A diagramatic representation of PVX clones, 3' of the bacteriophage T7 promoter and from which infectious transcripts can be made. The PVX-GFP clone contains the GFP gene inserted 3' of a duplicated coat protein (CP) promoter (a). The PVX.GFP-TGBp2 infectious clone contains GFP-TGBp2 fused genes inserted 3' of a duplicated CP promoter and the endogenous TGBp2 gene was deleted (represented in black box) (b). The PVX.TGBp3-GFP clone contains a GFP fusion inserted to TGBp3gene (c).

Replication of positive strand RNA viruses.

Replication of all positive strand RNA viruses is fundamentally similar. The virion enters a cell and the genomic RNA is uncoated. The RNA is translated to produce proteins required for virus replication. The viral replicase is typically anchored to cellular membranes and synthesizes complementary RNAs from the genomic RNA template (Buck, 1996; Schwartz *et al.*, 2002). The complementary RNAs act as templates for synthesis of new positive strand RNAs and sub-genomic RNAs. Sub-genomic RNAs are used for the translation of TGB proteins and the coat proteins, which are necessary for the virus movement and encapsidation (Angel *et al*., 1996; Lough *et al*., 2000; Baulcombe *et al*., 1995). A general schematic diagram for positive strand RNA virus replication is shown in Figure 2.

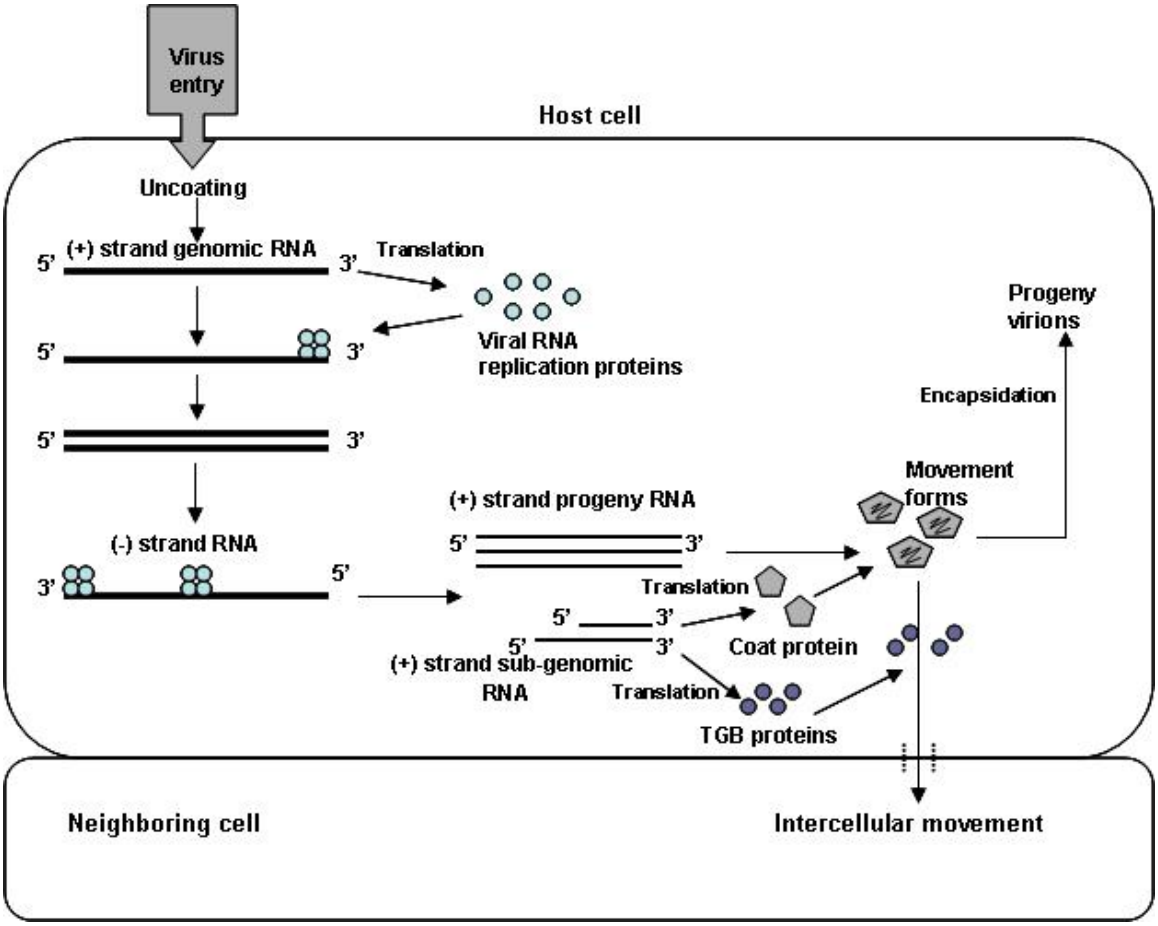

Fig 2: Schematic diagram for positive strand RNA virus replication.

The PVX replicase is a single protein which contains methyltransferase, helicase, and polymerase domains required for virus replication (Davenport and Baulcombe, 1997). The methyltransferase domain is responsible for capping the 5' end of the viral genome. The polymerase domain is responsible for new strand synthesis and the helicase domain is responsible for unwinding duplex RNA during new strand synthesis (Buck, 1996; Koonin and Dolja, 1993). Like many positive strand RNA viruses, PVX expresses these three domains on one protein (Buck, 1996).

For all positive strand RNA viruses, synthesis of the complementary RNAs initiates from the 3' terminus of the genomic RNA. The 3' untranslated region (3' UTR) is approximately 74 nucleotides in length, although this varies among potexviruses. The 3' UTR can fold into 3 stem loop structures but only the SL3 structure is known to be required for virus replication (Batten *et al*., 2003). The SL3 loop contains a hexanucleotide sequence (5'-ACUUAA) that is necessary for initiation of minus strand synthesis (Bancroft *et al*., 1991; Lough and Lucas, 2006). Mutations eliminating or altering this hexanucleotide sequence reduce minus strand synthesis (Batten *et al*., 2003; White *et al.,* 1992). There is also a conserved U-rich sequence (UAUUUUCU) located downstream of the hexanucleotide sequence which is also important for minus strand synthesis. It has been suggested that this U-rich sequence binds host factors that may be involved in virus replication. Cellular extracts were mixed with a PVX 3' end probe and host proteins were found to bind to the 3' end in gel retardation assays. The U-rich sequence was identified as a target for host factor binding, but the identity of these host factors is unknown (Pillai-Nair *et al*., 2003; Sriskanda *et al*., 1996).

This negative strand RNA acts as template strand for the synthesis of genomic and sub-genomic positive strand RNAs. It has been reported that the several cis-acting elements in the 5' UTR region are essential for synthesis of positive strands and sub-genomic RNAs (Kim and Hemenway, 1996). The 5' UTR is 84 nucleotides in length but there are elements that fold into two stem loop structures required for virus replication that extend to the first 182 nucleotides. The SL1 structure is required for synthesis of genomic and subgenomic RNAs. There are extensive single-stranded regions between SL1 and SL2. There are five ACCAA motifs repeated throughout the 5' UTR and which overlap with SL1 (Kim and Hemenway, 1996). These repeats bind 54 kDa cellular proteins (p54) which are also important for PVX RNA replication (Kim *et al.,* 2002). Since the ACCAA repeats overlap the SL1 structure, it is not clear whether the cellular protein recognizes the repeated elements specifically or the SL1 structure.

While there has been significant progress in defining the 5' and 3' structures regulating PVX replication, very little is known about which elements attract the PVX replicase and what proteins comprise the replication complex. It is also not understood where replication occurs inside the cell.

Role of cellular membranes in virus replication.

Recent studies showed that the replication of positive-sense strand RNA viruses involves association with cellular membranes. In many cases, virus infection induces invaginations of cellular membranes, forming vesicles which are associated with replication complexes. These vesicles can be derived from a variety of membranes. For example, the *Brome mosaic virus* (BMV), *Tobacco mosaic virus* (TMV) and *Cowpea*

mosaic virus (CPMV) replicases associate with invaginations of the ER (Restrepo-Hartwig and Ahlquist, 1996; Heinlein *et al.,* 1998; Reichel and Beachy, 1998; Carette *et al.*, 2000). The *Turnip yellow mosaic virus* (TYMV) and *Alfalfa mosaic virus* (AMV) replicases associate with the chloroplast outer membrane (Garnier *et al.*, 1986; deGraaf *et al.*, 1993). The *Cucumber mosaic virus* (CMV) replicase associates with vacuolar membranes (Hatta and Francki, 1981). The *Carnation italian ringspot virus* (CIRV) and the *Tobacco rattle virus* (TRV) replicases associate with mitochondria, while the *Pea enation mosaic virus* (PEMV) replicase associates with the nuclear envelope, and the *Tomato bushy stunt virus* (TBSV) replicase associates with peroxisomes (Rubino *et al.*, 1995; Harrison and Roberts, 1968; Demler *et al.*, 1994; Russo *et al.*, 1983; Lupo *et al.*, 1994).

Recent studies of BMV, TBSV, and TMV showed these viral replicases accumulate in membranous vesicles in yeast cells. Each of these viruses encodes two proteins which comprise the viral replicase. BMV is a tripartite RNA virus which encodes the 1a and 2a proteins on RNA1 and RNA2. The 1a protein contains membrane binding, methyltransferases, and helicase domains. The 2a protein has polymerase activity. The 1a protein recruits the 2a protein to the viral RNA. The replication complex assembles along the outer perinuclear ER. The BMV 1a protein induces inward invaginations of the ER and the replicase accumulates in vesicles inside the ER lumen (Schwartz *et al.,* 2002; Schwartz *et al.,* 2004). Assembly of the replication complex is necessary for formation of ER luminal vesicles (Schwartz *et al.,* 2004).

Assembly of the TBSV replication complex inside vesicles parallels BMV, although there are differences between these two viruses in their genome expression

strategies and sub-cellular location of their replicases. TBSV is a monopartite RNA virus which encodes the p33 and p92 proteins. The p92 protein is produced by readthrough of a translation stop codon at the 3' end of the p33 protein. The p33 protein has a membrane binding domain and an RNA binding motif. The p92 protein has polymerase activity. The p33 protein recruits the p92 protein to the viral RNA. The replication complex assembles along the peroxisomal boundary membrane. This is followed by extensive inward invagination of this membrane forming novel peroxisomal vesicular bodies (pMVBs) (Martelli *et al*., 1998). These pMVBs fill the interior of the peroxisomes (Appiano *et al*., 1983, 1986) in yeast cells.

TMV is similar to BMV because its replication complex forms along the ER network. TMV is a monopartite RNA virus which encodes the 126 kDa and 183 kDa proteins. The 183 kDa protein is produced by readthrough of a translational stop codon at the 3' end of the 126 kDa ORF. Both 126 kDa and 183 kDa proteins have helicase and methyl transferase domains, but the 183 kDa protein has the polymerase active site (Goregoaker *et al*., 2001; Watanabe *et al*., 1999). Assembly of the TMV replicase along the ER network and invagination of these membranes has not been studied as extensively as BMV and TBSV. However, replicase containing vesicles have been identified in TMV infected cells. The TMV MP and CP also associate with these complexes. It has been recently reported that viral replicase containing complexes move along the microfilament network to the periphery of the cell and sometimes these membrane containing replication complexes move across plasmodesmata (Liu *et al*., 2005; Kawakami *et al.,* 2004). Thus, for TMV the membrane bound replicase serve as a vehicle for trafficking virus between neighboring cells.

PVX and cellular membranes.

Current studies of PVX show the TGBp2 and TGBp3 protein associate with the ER and this association is important for virus movement (Mitra *et al*., 2003; Krishnamurthy *et al*., 2003). TGBp2 causes invagination of the ER network and the resulting vesicles play a role in virus cell-to-cell movement (Ju *et al*., 2005). The contents of the TGBp2 induced vesicles are not known. Vesicles may contain viral RNA and/or viral proteins.

In this study, we are interested to determine the sub-cellular location and membrane association of the PVX replicase. These data are important for understanding how the PVX life-cycle progresses in infected cells. We are also interested to learn if subcellular accumulation of the PVX replicase resembles the BMV, TBSV, or TMV models. Does the PVX replicase associate with the ER, with vesicles, or with movement factors? This investigation will also determine if there is a possibility that the replicase may be a factor that is transported between cells based on its association with viral movement proteins.

Chapter III

EXPERIMENTAL DESIGN AND METHODOLOGY

Infectious clones and plasmids.

PVX-GFP, PVX.GFP-TGBp2, and PVX.TGBp3-GFP are infectious clones of PVX containing the bacteriophage T7 promoter and GFP gene inserted into the PVX cDNA and was described in prior studies (Figure1; Verchot *et al*., 1998; Krishnamurthy *et al.,* 2003; Mitra *et al*., 2003). The pRTL2 plasmids containing the *Cauliflower mosaic virus* (CaMV) 35S promoter and GFP or CFP fused to PVX TGBp2, TGBp3, or an ER targeting signal were used extensively in previous studies (Ju *et al*., 2005, Samuels *et al*., 2007, and Ju *et al*., 2008) All plasmids were maintained in *Escherichia coli* strain JM109 (Sambrook *et al*., 1989).

The Pure Yield Plasmid Midi Prep System ^{TM} (Promega, Madison, WI) was used to extract plasmid DNA from *E. coli* grown in LB media plus ampicillin (50 μg/ml) at 37^{o}C for 16-18 hours. Cultures were centrifuged at 10,000 g for 10 minutes, and the supernatant was discarded, and tubes were drained on a paper towel to remove the excess media. Cell pellets were resuspended in 3 ml of cell resuspension solution. Three ml of cell lysis solution was added, and the samples were inverted gently for three to five times. Mixtures were incubated for 3 minutes at room temperature (22-25^{o}C). Five ml of

neutralization solution was added, and Lysate were mixed by gentle inversion. Lysates were allowed to incubate for 2-3 minutes in an upright position and then centrifuged at 14,000 g for 30 minutes. Pure Yield™ Clearing Columns were placed into 50 ml disposable plastic tubes. The supernatants were poured into the column and incubated for 2 minutes to allow the cellular debris to rise to the top. Pure Yield™ Clearing Columns were centrifuged at 1,500 g for 5 minutes. Pure Yield™ Binding Columns were placed into new 50 ml disposable plastic tubes and filtered lysates were poured into each tube. Columns were centrifuged at 1,500 g for 3 minutes. Five ml of endotoxin removal wash Solution (with added isopropanol) was added to each Pure Yield™ Binding Columns, and then centrifuged at 1,500 g for 3 minutes. Flows through fractions were discarded. Twenty ml of column wash solution (with added ethanol) was added to the binding columns and centrifuged at 1,500 g for 5 minutes. The flow through was discarded, and the columns were centrifuged at 1,500 g for an additional 10 minutes to ensure the removal of ethanol. The binding columns were placed in new 50 ml disposable plastic tubes. DNA was eluted by adding 800 µl of nuclease free water to the binding columns and centrifuged at 1,500 g for 5 minutes. The filtrate was collected from the 50 ml tube and transferred to a 1.5 ml eppendorf tube. Quantity and purity of the DNA yield was measured by using a Nanodrop ND-1000 spectrophotometer (Innovadyne Technologies Inc., Santa Rosa, CA) and by 1% agarose gel electrophoresis and staining.

***In vitro* transcription.**

Twenty five µg of PVX-GFP, PVX.GFP-TGBp2, or PVX.TGBp3-GFP containing plasmid were digested for 3 hours at 37°C with 4µl of *SpeI* restriction enzyme

(New England Biolabs, Ipswich, MA), 10 µl of 10X buffer 2, 1 µl of 100X BSA, and nuclease free water. DNA digestion was verified using 1% agarose gel electrophoresis and staining. Digested DNA was stored at -20^{o}C.

One µg of linearized DNA was transcribed using the mMESSAGE mMACHINE^{TM} kit (Ambion Inc., Austin, TX). Ten µl of 2X NTP/CAP, 2 µl of 10X reaction buffer, 2 µl of enzyme mix were added to the DNA on ice and the mixture was incubated for 10 minutes at 37^{o}C. Two µl of GTP was added to the mixture and again incubated for 2 hours at 37^{o}C. Transcription results were viewed by 1% agarose gel electrophoresis and EtBr staining. The transcription reaction was quantified using a Nanodrop ND-1000 spectrophotometer.

BY-2 protoplast preparation & transfection.

Suspension cells of tobacco BY-2 cells (Nagata *et al*., 1992) were maintained as described previously (Ju *et al*., 2005). BY-2 cells were propagated in the BY-2 culture medium (Murashige and Skoog medium [Murashige and Skoog salts; Sigma-Aldrich Co., St. Louis, MO] supplemented with 30 g/l of sucrose, 256 mg/l KH_2PO_4, 100 mg/l myoinositol, 1 mg/l thiamine and 0.2 mg/l 2, 4-dichlorophenoxyacetic acid, pH 5.5 (w/v)) on a rotary shaker at 120 rpm at 28^{o}C in the dark. Two ml of BY-2 cells were transferred to 50 ml of fresh media every 4 days.

For protoplast preparation, 3 to 5 day-old cultures were collected by centrifugation at 59g for 5 minutes. Cells were resuspended in enzyme solution (1.5% Onozuka R10 cellulase [w/v; Yakult Pharmaceutical, Tokyo, JP], 0.2% macerase [w/v; Calbiochem-Novabiochem, La Jolla, CA], 0.45 M mannitol, and 3.6 mM 2-(N-

morpholino) ethane sulfonic acid [MES], pH 5.5). Cells were digested for 3 to 5 hours at 30^{o}C while gently shaking at 108 rpm on a rotary shaker. The protoplasts were separated from cellular debris by filtration through two 41 μl nylon mesh (Spectrum laboratories, Rancho Dominguez, CA) into a 600 ml beaker and transferred into two 50 ml centrifuge tubes. The filtrate containing protoplasts, was centrifuged at 59g for 5 minutes and washed twice with solution I (0.5 M mannitol, 3.6 mM MES, pH 5.5 [w/v]) at 59g for 5 minutes. Finally protoplasts were resuspended in 5 ml of solution II (0.45 M mannitol, 3.6 mM MES pH 5.5, and 0.1mM $CaCl_2$) and placed on ice for one hour. Fifty μl protoplasts were mixed with 100 μl of 0.1% fluoroscein diacetate, incubated for 5 minutes, and the counted using a haemocytometer. The total number of protoplasts was determined using the following equation: mean cells per 20 μl x 10,000 x dilution factor x total volume. The final volume of the protoplast mixture was adjusted to make 1 x 10^6 protoplasts/ml.

For DNA or RNA transfection, 500 μl of protoplasts were mixed with 5-10 μl of PVX-GFP, PVX.GFP-TGBp2, or PVX.TGBp3-GFP transcripts and 200 μl of solution II and placed in a 0.4 cm gap cuvettes (Bio-Rad Laboratories, Hercules, CA) on ice. Electroporation was carried out at 0.25 KV, 100 Ω and 125 μF using a BioRad Gene Pulser (Bio-Rad Laboratories). Following electroporation, protoplasts were immediately transferred into a new eppendorf tube containing 800 μl of solution II and incubated on ice for 30 minutes. Protoplasts were collected by centrifugation at 59g for 5 minutes, resuspended in 1 ml of BY-2 culture media plus 0.45 M mannitol and transferred to 6-well cell culture plates (Becton Dickinson Labware, Franklin Lakes, NJ). The culture plates were coated with a solution of BY-2 culture media plus 0.45 M mannitol and

1% agarose (w/v; pH 5.7). Protoplast samples were cultured at 27- 28 ^{o}C in dark and collected at early (12 or 18 hpi), and later (36 or 48 hpi) stages of infection, for immunofluorescence labeling.

Immunofluorescence labeling of protoplasts.

Experiments were conducted to determine if GFP fluorescence colocalizes with immunofluorescence detecting the PVX replicase. Immunofluorescence labeling of protoplasts was performed as described in Liu *et al.* (2005). To prepare slides, protoplasts were collected by centrifugation at 59g for 5 minutes. Supernatant was discarded and pellet was washed twice with PHEM buffer (60mM PIPES, 25mM HEPES, 5mM EGTA, 2 mM $MgCl_2$, pH 6.9) then resuspended in 500 µl fixative (2% [v/v] paraformaldehyde and 0.5% [v/v] DMSO in PHEM buffer) for 15 minutes at room temperature. Fixed protoplasts were centrifuged at 59g for 5 minutes and the pellet was washed twice with PHEM buffer. Following the last wash a small amount of PHEM was left with the pellet, mixed gently, and then transferred onto a cover glass. The cover glass was left for 30 minutes in a sterile hood. A thin film of 0.7% Bacto-agar (dissolved in PHEM) was placed on the dried cover glass using a square-shaped wire loop. Then PHEM was added on top of the cover glass. Excess buffer was blotted, 200 µl of 1% Triton X-100 (in PHEM) was added, and the cover glass was kept for 10 minutes at room temperature. Excess solution was blotted and the cover glass was washed thrice for 3 minutes with PHEM. Then $NaBH_4$ was added to the cover glass, incubated for 10 minutes at room temperature, and then washed 3 times with PHEM. Ice cold methanol was added,

incubated for 10 minutes at room temperature, and then washed thrice for 5 minutes with PHEM. PHEM was removed by blotting and cover glass was left to air dry.

For immunolabeling, cover glasses were incubated overnight with PVX replicase goat antisera obtained from Cindy Hemenway (NC State University) (diluted 1:500) in a moisture chamber at 4^{o}C. Then cover glasses were washed five times for 5 minutes with PHEM. Then Alexa Fluor 633 conjugated secondary antisera (Molecular Probes, Inc., Eugene, OR.) was diluted 1:100 in PHEM, added to the cover glass, and incubated for 2 hours in a moisture chamber at room temperature. Cover glasses were washed five times for 5 minutes with PHEM and then mounted on a slide with commercially available Vectashield^{TM} mounting media (Vector Laboratories, Inc., Burlingame, CA).

Plants, plant inoculation, and plasmid bombardment.

Nicotiana benthamiana plants were used in all experiments. Infectious transcripts of PVX-GFP, PVX.GFP-TGBp2, and PVX.TGBp3-GFP were prepared as described in the previous objective. The leaves of *N. benthamiana* were dusted with cellite powder and rub inoculated with transcripts. Two leaves per plant were treated, each with 5 µl of transcript. Non-inoculated control plants were treated similarly with 5 µl of ddH_2O. GFP fluorescent PVX infection foci were identified 3 days post inoculation (dpi) using a Nikon E600 epifluorescence microscope (Nikon USA Inc., Dallas, TX) and were excised for experiments involving immunofluorescence or immunogold labeling.

Leaves were also bombarded with pRTL2 plasmids expressing GFP or CFP fusions and then directly imaged using confocal microscopy. Plasmid bombardments were conducted as described in Samuels *et al*. (2007).

Immunofluorescence labeling of PVX infected plants.

Experiments were conducted to determine if GFP or GFP fusions co-localize with immunofluorescence detecting either the PVX replicase or the ER resident marker protein disulfide isomerase (PDI). Leaf segments containing fluorescent infection sites were fixed in eppendorf tubes with a solution of 3.7% (v/v) formaldehyde, 5% (v/v) dimethyl sulfoxide, and PHEM buffer for 2 hours as in Liu *et al.* (2005). Leaf segments were washed thrice with PHEM (3 minutes/each wash) between each step in the procedure. Fixed segments were placed on microscope slides and digested with cell wall degrading enzymes (1% Onozuka R10 cellulase, 0.1% pectolyase [Kikkoman, Tokyo, JP] and 0.1% bovine serum albumin [BSA; fraction V] in PHEM buffer) for 2 hours. Following washes the segments were incubated with 1% (v/v) Triton X-100 for 20 minutes, and then incubated with ice cold methanol for 10 minutes. Following washes the segments were incubated overnight in a moisture chamber at 4^{o}C with PVX replicase (diluted 1:100) or PDI (Rose Biotechnology, San Francisco, CA) antisera. Immunolabelling was conducted as for protoplasts (Liu *et al*., 2005).

Fixation and LR-White or Spurr's resin embedding of plant materials.

Virus-infected and mock-inoculated leaf segments were harvested at 5 dpi and subjected to either cryo-fixation (conducted at Oklahoma Medical Research Foundation (OMRF) with the assistance of Ben Fowler) and embedding in LR-White or, chemical fixation and embedding in Spurr's resin (embedding in LR-White or Spurr's resin was conducted by Terry Colberg at OSU).

Cryo-fixation and LR-White embedding was carried out as previously described for virus infected leaves (Ju *et al*., 2005; Kiss *et al.,* 1990). Leaf segments were washed with distilled deionized water (ddH_2O) and were fitted into 0.4-mm freezer hats (Ted Pella, Reading, CA) filled with lecithin solution (100 mg/ml in chloroform). A drop of 15% (w/v) aqueous dextran (M_r 38,800) was added to each freezer hat. Freezer hats were loaded onto a holder and inserted into the Balzer HPM010 high-pressure freezing machine (Manchester, NH) and immediately transferred into Nalgene (Rochester, NY) cryogenic vials containing super cooled 100% acetone which were located in a liquid nitrogen bath. Freeze substitution was carried out by transferring samples from the freezer hats to a solution of 1% OsO_4 and acetone. Samples were maintained in a dry ice/acetone bath for 2.5 days at −78.6°C. Samples were transferred from the freezer hats to vials of acetone and incubated in a freezer at −20°C for 2 hours, then to a refrigerator at 0°C for 2 hours, and then on the lab bench (23°C) for 2 hours. Samples in vials were then rinsed three times in acetone for 20 minutes, three times in 100% ethanol for 20 minutes, and embedded in LR White resin.

Stepwise chemical fixation was carried out as described by Dunoyer *et al*. (2002). Leaf segments were pre-incubated with 1% glutaraldehyde in 25 mM potassium phosphate buffer (pH 7.4) for one hour in a bench top vaccum chamber and then immersed in a primary fixative [2% (vol/vol) glutaraldehyde, 0.1 ml of saturated picric acid in 25 mM potassium phosphate buffer (pH 7.4)] for 15 minutes at room temperature. Segments were incubated at 4^{o}C for 16 hours, were washed four times (five minutes per wash) in 25 mM PIPES buffer (pH 7.0) and then transferred into secondary fixatives [2% (wt/vol) OsO_4 and 0.5% (wt/vol) potassium ferrocyanide in 25 mM PIPES buffer (pH

7.0)] for 2 hours at room temperature. Then samples were washed twice with 25 mM PIPES buffer (pH 7.0) for 15 minutes and then twice with ddH_2O for another 15 minutes. Samples were transferred to 2% (wt/vol) aqueous uranyl acetate for 16 hours at 4^oC and washed twice with ddH_2O for 15 minutes. Samples were dehydrated in an acetone series (10, 20, 40, 60, 80, and 100%) and infiltrated with acetone/Spurr's resin (1:1) overnight and then embedded in Spurr's resin.

Ultra thin sections (700 nm) of LR-White or Spurr's resin embedded samples were cut using a diamond knife on a Sorvall MT 6000 ultra microtome. Sections were mounted on formvar-coated nickel grids (Electron Microscopy Science, Hatfield, PA) and used for immunogold labeling.

Immunogold labeling of LR-White or Spurr's resin-embedded plant material.

Immunogold labeling of tissues were conducted using monoclonal GFP (BD Living Colors^{TM}; Clontech Laboratories, Mountain View, CA) and PVX replicase polyclonal goat antisera. Grids were incubated in blocking solution consisting of PBS, pH 7.5 (130 mM NaCl, 7.0 mM Na_2HPO_4, 3.0 mM NaH_2PO_4) plus 2% BSA (w/v) for 15 minutes, and then was incubated with 5% normal sheep sera (Sigma-Aldrich Co.) in PBS plus 2% BSA for 15 minutes. Then samples were incubated with GFP monoclonal antisera diluted 1:500 in PBS plus 2% BSA (w/v), PVX replicase goat antisera diluted 1:500 in PBS plus 0.1% Tween (v/v), or buffer containing no primary antisera for 2 hours. Grids were then washed five times for 5 minutes with PBS and then with PBS plus 2% fish gelatin (v/v) for 15 minutes. Grids were then incubated for 1 hour with either 10

or 20 nm gold-conjugated goat antisera (EY Labs, San Mateo, CA) diluted 1:10 in PBS plus 2% fish gelatin.

Some grids were dual labeled with antiserum to detect replicase and GFP and a longer procedure was followed. Grids were first incubated with replicase goat antisera diluted 1:500 in PBS plus 0.1% Tween (v/v) for 2 hours and then with the 20 nm gold-conjugated rabbit anti-goat serum diluted 1:10 in PBS plus 2% fish gelatin for 2 hours as described above. Samples were washed twice for 10 minutes with PBS and then incubated for 30 minutes with GFP monoclonal antisera diluted 1:500 in PBS. Grids were washed five times for 5 min with PBS, then for 15 min with PBS with 2% fish gelatin, and were incubated 30 min with 10 nm gold-conjugated goat anti-mouse serum (EY Labs) diluted 1:10 in PBS plus 2% fish gelatin.

Grids were washed three times for 5 minutes with ddH_2O, and stained with a solution of 2.5% uranyl acetate and 70% methanol (v/v) for 30 minutes, and then with a solution of 2% Reynold's lead citrate pH 12.0 (in ddH_2O) for 20 minutes. Samples were washed with mildly warm ddH_2O three times for 5 minutes and then dried.

Spurr's resin embedded sections were consecutively labeled with PVX replicase goat primary, anti-goat secondary and GRP78 (BiP) rabbit primary and anti-rabbit secondary antisera (ABR-Affinity Bioreagents, CO). Procedure for dual labelling of LR White-embedded plant material was followed.

Staining of grids with uranyl acetate and Reynold's lead citrate

A petri dish was lined with a parafilm and one drop of uranyl acetate (EM Sciences, PA) per grid was placed on the parafilm. (Stains were stored in dark bottles.)

Grids were dipped in water and inserted into uranyl acetate drop, section side up and stained for 30 minutes. Grids were rinsed with ddH_2O for 2 minutes and blot dried with a filter paper. One half of a partitioned petri dish was lined with a parafilm and other side was filled with NaOH and CO_2 free ddH_2O in order to make a CO_2 free chamber. One drop of lead citrate (lead nitrate and sodium citrate (Sigma-Aldrich Co., St. Louis, MO) per grid was placed on the parafilm. Grids were dipped in CO_2 free ddH_2O and inserted into lead citrate drop, section side up and stained for 20 minutes. Grids were rinsed with CO_2 free ddH_2O for 2 minutes and blot dried with a filter paper.

Laser scanning confocal microscopy and transmission electron microscopy.

A Leica DMRE microscope with Leica TCS SP2 confocal imaging system was used for imaging the immunolabelled tissues. Ar/Kr lasers were used for detecting GFP and He/Ne lasers for detecting Alexa Fluor 633 fluorescence. Alexa Fluor 633 conjugates (Molecular Probes, Inc., Eugene, OR.) are bright and photostable, and have peak absorption centered at 632 nm and a peak emission at 650 nm. Images were recorded and compiled using Adobe Photoshop CS software (Adobe Systems, San Jose, CA).

Electron microscopic analysis of samples was carried out using a JEOL JEM-2100 Scanning Transmission Electron Microscope System with an EDAX Genesis 2000 EDS system (JEOL Ltd., Tokyo, Japan)

Electron microscopic images were taken, and number of gold particles labeling specific structural components of the cell was scored in 10 μm^2 fields (using an ultrastructure size calculator) or in each organelle. Gold particles in each field/organelle were counted manually. Average and standard error was calculated and tabulated.

Sucrose gradient fraction of plant extracts containing PVX replicase.

Forty g of PVX.TGBp3-GFP infected *N. benthamiana* leaves were collected from plants at 14 dpi and then homogenized in 100 ml of ice-cold buffer A [50 mM Tris-HCl, pH 8.2; 15mM $MgCl_2$, 120 mM KCl, 20% glycerol, 1 mM DTT, 5 mM EDTA and 10 µl/ml of Protease Inhibitor Cocktail for plant cell and tissue extracts™ (Sigma-Aldrich Co., St. Louis, MO) added just before use] in a waring blender. The crude homogenate was filtered through gauze and miracloth (Calbiochem, La Jolla, CA) into a fresh tube and centrifuged at 500g for 10 minutes at 4°C. The supernatant was removed and centrifuged at 30,000g for 30 minutes using a SW 32.1 ultracentrifuge rotor and Optima™ L-XP Series preparative ultracentrifuge (Beckman Coulter, Inc., Fullerton, Cal.). The resulting pellet was resuspended in 6 ml buffer B (50 mM Tris-HCl, pH 8.2; 15 mM $MgCl_2$, 5% glycerol, 1 mM DTT, 5 mM EDTA and 10 µl/ml of Protease Inhibitor Cocktail) and divided into 3 ml samples and stored in liquid N_2. Each thawed sample was loaded onto 7.5 ml, 20-60 % continuous sucrose gradients. After centrifugation at 189,000g for one hour at 4°C, 0.5 ml fractions were collected from the top of each gradient. Approximately 16 to 18 fractions were collected per gradient and then stored in liquid N_2 (Plante *et al.*, 2000).

Protein gel electrophoresis and immunoblot analysis of concentrated sucrose gradient fractions.

Gradient fractions were concentrated five fold according to Wessel and Flugge (1984). A 0.2 ml of each fraction was combined with 0.8 ml of methanol and then mixed by vortexing and low speed centrifugation at 9,000g for 10 seconds. Then 0.2 ml of

chloroform was added and samples were mixed again. Finally 0.6 ml of water was added and samples were mixed again and centrifuged at 9,000g for 1 minute. The aqueous phase was discarded and 0.6 ml of methanol was added to the lower chloroform phase and the inter-phase which has precipitated protein. Samples were mixed and centrifuged again at 9,000g for 2 minutes to pellet the protein. The supernatant was removed and the protein pellet was dried for 15 minutes under a stream of air.

The dried pellets were diluted in 40 µl protein dissociation buffer (100 mM Tris-HCl pH 7.5, 10 mM KCl, 5 mM $MgCl_2$, 0.4M sucrose, 10% glycerol, and 10 mM β-mercaptoethanol; Sambrook *et al*., 1989) and boiled for 5-10 minutes. Samples were centrifuged for 5 minutes at 3,000g and loaded onto 12.5% SDS-polyacrylamide gels which were run at 100 V for 3 hours. Vertical transfer of denatured proteins onto nitrocellulose membranes (Perkin Elmer, Boston, MA) was conducted using a BioRad Trans-Blot apparatus (BioRad Laboratories, Hercules, CA) at 100V for 1.5 hours at 4^{o}C.

Since replicase antisera detected only intact non-denatured proteins, 150 µl unconcentrated fractions plus 50 µl protein dissociation buffer were applied directly to a nitrocellulose membrane using a Bio-Dot SF apparatus (Bio Rad, Hercules, CA). To assemble the apparatus the nitrocellulose membrane and three 3MM chromatography papers were prewetted with PBS, 0.1% Tween for 10 minutes and then layered inside the apparatus. Air bubbles were removed, vacuum was applied, and then pins were tightened to prevent the cross contamination. Membrane was re-hydrated with 100 µl of PBS plus 0.1% Tween per well. Samples were allowed to filter through the membrane gently and then the wells were washed with 200 µl of PBS plus 0.1% Tween. The membrane was

allowed to completely dry and then was removed from the apparatus before turning off the vacuum. Membranes were used for immunoblot analysis.

The ECL-Plus Chemiluminescence Immunodetection System (GE healthcare UK limited, Buckinghamshire, UK) was used for all protein blots. Membranes that were stored at 4^{o}C in a plastic wrap were pre-wetted in ddH_2O for 5 minutes. Membranes were incubated in PBS, 0.1% Tween, plus 2.5% nonfat dry milk for 1 hour, washed three times for 10 minutes with PBS plus 0.1% Tween and incubated 1 hour with primary antisera. Membranes were probed with PVX replicase goat polyclonal or commercially available GFP monoclonal or BiP (GRP 78) rabbit polyclonal antiserum. In addition, membranes were probed with *Arabidopsis thaliana* SEC12 (AtSEC12), AtSYP61, AtSYP21, and AtSYP41 rabbit polyclonal antiserum obtained from Dr. A. Sanderfoot at University of Minnesota (Bar- Peled and Raikhel 1997; Sanderfoot *et al.*, 1999; Bassham *et al.*, 2000) to determine if these cellular proteins reside in the same fractions as the PVX proteins. Blots were washed three times for 5 minutes with PBS plus 0.1% Tween and treated with horseradish peroxidase conjugated secondary antiserum, diluted 1:10,000 in PBS containing 2.5% nonfat dry milk for 1 hour. Membranes were washed three times for 10 minutes, developed using the Western Lightning Chemiluminescence reagent plus developer (Perkin Elmer, Boston, MA), and then exposed to Kodak bio max light film (Kodak, Rochester, NY).

Densitometry was used to study changes in band intensities across the auto-radiographs for each immunoblot and to compare protein distributions in fractions of PVX.TGBp3-GFP infected and healthy leaf protein extracts. Density values were calculated using the Fluor Chem software. For each autoradiograph, the background was

automatically subtracted by determining the average of the 10 lowest pixel values surrounding each individual band. For a more rigorous quantification of the data, the density values for an empty lane was calculated and subtracted from each density value recorded for lane 1-16. The final values are presented as relative density values (RDV) and were plotted using Microsoft Excel 2003.

CHAPTER IV

RESULTS AND FINDINGS

Sub-cellular localization of the PVX replicase during infection in plants.

Mitra *et al.* (2003), Krishnamurthy *et al.* (2003), Ju *et al*. (2005), and Samuels *et al*. (2007) reported that PVX TGBp2 and TGBp3 associate with the ER and ER-derived vesicles. Confocal images shown in Figure 3 are to substantiate these prior reports. First, the GFP ORF was fused to an ER targeting and retention signal and inserted into plasmids 3' of CaMV 35S promoter (Haseloff *et al*., 1997). These plasmids were bombarded to tobacco leaf epidermal cells. Confocal microscopy revealed the typical reticulate tubular pattern indicative of the ER network (Figure 3A). PVX TGBp2 and TGBp3 were each fused to GFP and inserted into plasmids that were bombarded to tobacco leaf epidermal cells. As described in above mentioned studies, TGBp3-GFP is observed in the same reticulate network observed in GFP-ER expressing cells (Figure 3B). Tubular elements are sometimes shorter in TGBp3-GFP expressing cells and ER cisternae are often seen at vertices of the network. GFP-TGBp2 in contrast is often seen in vesicles (Figure 3C).

Plasmids containing CFP fused to TGBp2 and TGBp3-GFP fusions were co-bombarded to tobacco leaves. Confocal images of epidermal cells show that these fusion proteins co-localize in vesicles and along the ER network (Figure 3D, E, and F). For further comparison, the GFP fusions were introduced into the PVX genome (Figure 1).

The images here show that both proteins have a high affinity for the ER and associated vesicles (Figure 3G and H) during virus infection.

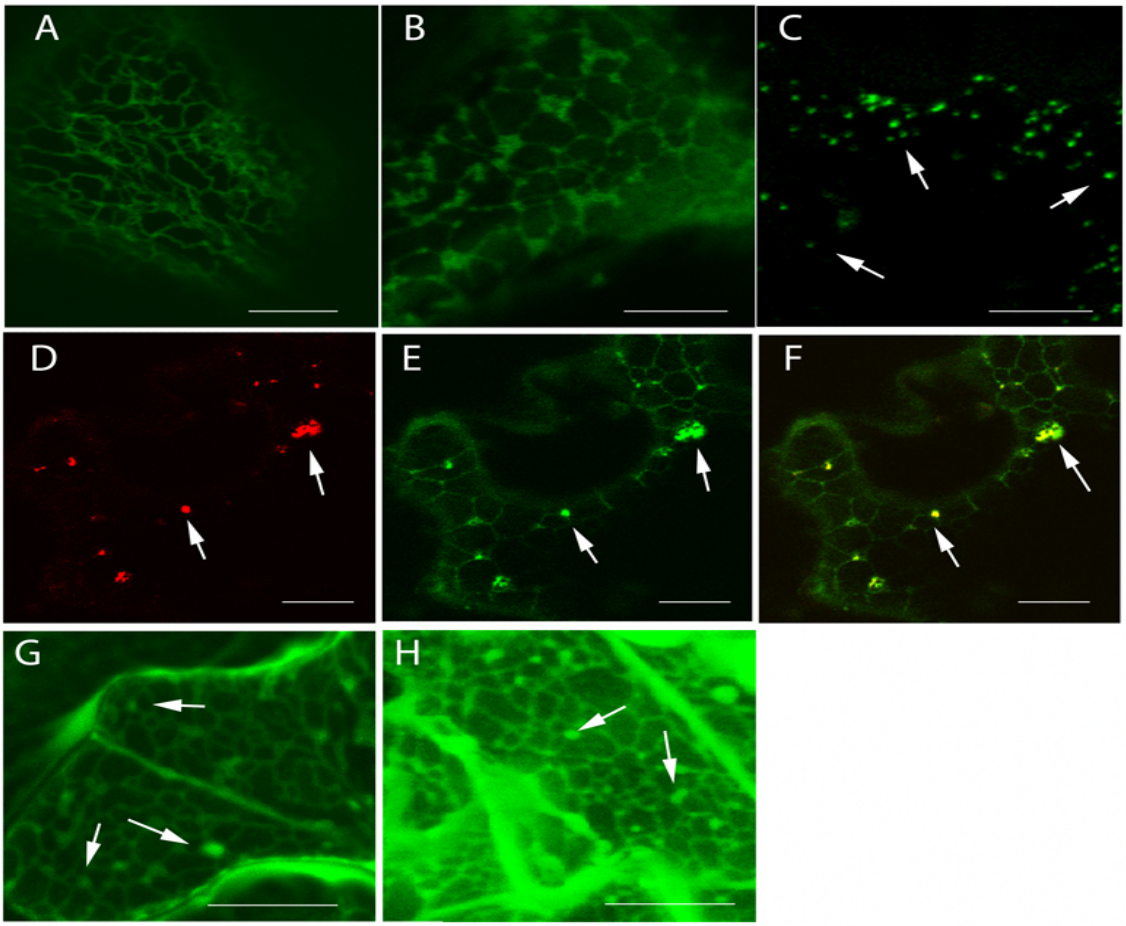

Figure 3: Confocal images of epidermal cells expressing (A) GFP-ER; (B) TGBp3-GFP; (C) GFP-TGBp2; (D, E, and F) CFP-TGBp2, TGBp3-GFP, and an overlay. Fluorescence due to CFP-TGBp2 is presented in red pseudocolor. The overlaid images show yellow where proteins co-localize. (G, H) PVX.GFP-TGBp2 and PVX.TGBp3-GFP infected cells respectively. Arrows in all panels point to examples of virus-induced vesicles. Bars represent 10 μm.

Plante *et al.* (2000) determined that the PVX replicase is membrane bound and developed a method to solubilize the template dependent PVX replicase. In this study, we conducted experiments to determine if the PVX replicase colocalizes with PVX TGBp2 and TGBp3 along the ER or ER-associated vesicles in PVX.GFP-TGBp2 and PVX.TGBp3-GFP infected cells. Transcripts derived from PVX.GFP-TGBp2 and PVX.TGBp3-GFP plasmids were used to inoculate *N. benthamiana* plants. GFP fluorescence was first seen in single cells at 3 dpi and by 7 dpi infection foci were typically 10-15 cells in diameter. Transverse sections of fluorescent foci harvested at 7 and 12 dpi were immunolabelled using PVX replicase antisera followed by Alexa Fluor 633 conjugated secondary antisera while GFP fluorescence was used to identify the TGBp2 and TGBp3 proteins in epidermal and mesophyll tissues. Immunolabelled tissues were viewed using confocal microscopy and the results were compared to determine if protein accumulation in each cell layer changed with time. Regardless of when foci were harvested the results were the same for each virus.

Among PVX.GFP-TGBp2 and PVX.TGBp3-GFP infected epidermal cells treated with replicase antisera, green fluorescent vesicles (Figure 4A and D) co-label with red fluorescence (Figure 4B and E) indicating the presence of PVX replicase. All vesicles which co-label with green and red fluorescence appear yellow in the overlaid images (Figure 4C, F).

In PVX.TGBp3-GFP infected epidermal cells, perforated sheets of cisternae ER are seen following treatment with fixative and cell wall degrading enzymes rather than the tubular network commonly seen in untreated cells (compare Figure 3A with Figure 4D and F). These perforated sheets typically lie deeper in the cell than tubular ER (Ridge

et al., 1999). Most confocal imaging of the tubular network focuses near the cell surface where imaging is easiest. The perforated sheets described by Ridge *et al.* (1999) are highly dynamic and change significantly with the streaming cytoplasm making it more difficult to image in cells that are not treated with fixative.

Figure 4G-I show fluorescence due to PVX.TGBp3-GFP in palisade mesophyll where there are an abundance of chloroplasts. The ER is compressed by the vacuole and chloroplasts making it difficult to characterize ER architecture. Vesicles that co-label with green and red fluorescence are abundant in these cells (Figure 4G-I). The overlaid images show that red and green fluorescence co- localize in the ER and vesicles indicating that TGBp3-GFP, and replicase localize.

Prior studies reported that GFP-TGBp2 induces novel vesicles to form from the ER (Ju *et al*., 2005, 2007). These vesicles were examined using confocal and electron microscopy and were shown to contain ribosomes and label with BiP antisera (an ER localized chaperone). To determine if the vesicles seen in this study are also ER-derived structures, PVX.TGBp3-GFP infected cells were treated with antisera detecting another ER localized chaperone: protein disulfide isomerase (PDI). Figure 4J, K, L are views of spongy mesophyll cells with large air spaces between cells. Green fluorescence (Figure 4 J) and red fluorescence (Figure 4K) are seen in vesicles. The yellow fluorescent vesicles in Figure 4L show that all TGBp3-GFP containing vesicles also contain PDI and are likely ER-derived. To verify non specific labelling, mock inoculated plants were also treated with replicase antisera. Figure 4M is a transmitted image of a mesophyll cell. Green and red fluorescence were not detected in control samples (Figures 4N and O) indicating that antiserum binding is specific to PVX infected tissues.

These preliminary experiments show that all epidermal and mesophyll cells contain replicase, GFP-TGBp2 and TGBp3-GFP along the ER network and ER-derived vesicles. To further test this hypothesis, immunofluorescence labeling was conducted in virus infected BY-2 protoplasts.

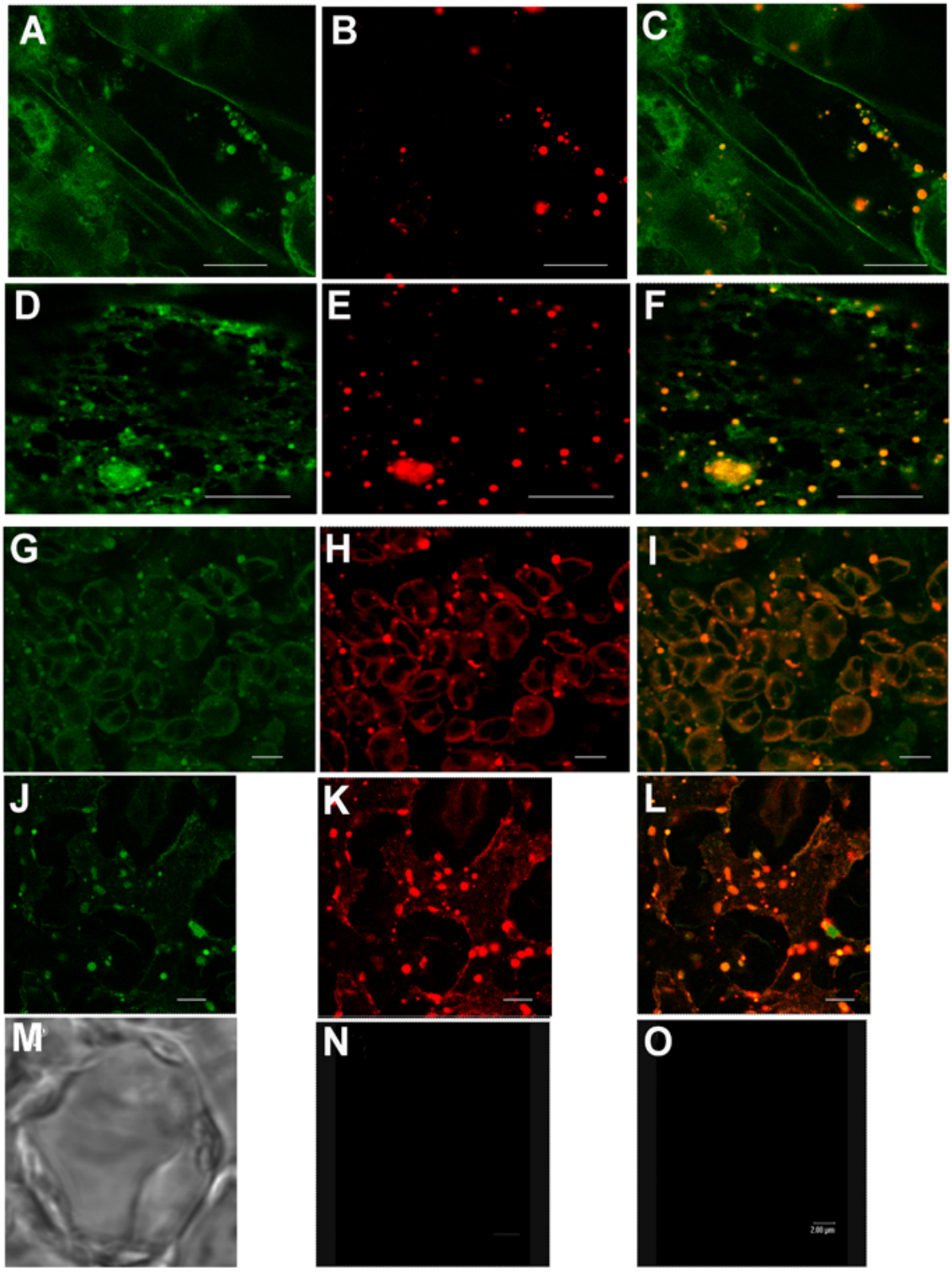
A
B
C
D
E
F
G
H
I
J
K
L
M
N
O

Figure 4: Confocal images of transverse sections of virus infected tobacco leaves. Show epidermal [A-C (7 days post inoculation (dpi)) D-F (12 dpi)], palisade mesophyll (G-I (7 dpi)) and spongy mesophyll (J-L (9 dpi)). Green fluorescence indicates GFP-TGBp2 (A) or TGBp3-GFP (D, G, J). Red fluorescence indicates replicase (B, E, H) or PDI (K). Yellow indicates where red and green overlap indicating proteins co-localize. Panels with no signals (M-O) are for mock inoculated protoplasts. Bars represent 10 μm. All images were taken using Kr/Ar laser set at 400 Hz and PMT detector within a 400 – 510 value range where chloroplast autofluorescence is not detectable as seen in panels N and O.

Subcellular localization of the PVX replicase, GFP-TGBp2, and TGBp3-GFP during infection in protoplast.

Protoplasts were prepared from BY-2 suspension cells and transfected with pRTL2-GFP-TGBp2, pRTL2-TGBp3-GFP, or -GFP-ER plasmids or inoculated with PVX-GFP, PVX.GFP-TGBp2, and PVX.TGBp3-GFP infectious transcripts (Figure 1) and immunofluorescence labeling was conducted, as in leaves. Protoplasts offer the advantage of studying viral protein accumulation in synchronously infected cells. Thus we can survey viral protein accumulation at specific times during the infection cycle. Since GFP fluorescence is first seen at 12 hpi, protoplasts were harvested at intervals between 12 and 48 hpi to determine if protein sub-cellular accumulation and co-localization is time-dependent. Protoplasts were inoculated with PVX.GFP-TGBp2 and PVX.TGBp3-GFP and then were harvested at early (12 or 18 hpi) and late (36 or 48 hpi) stages of virus infection (Figure 5). Protoplasts were then fixed onto cover glasses and immunolabelled with PVX replicase polyclonal and GFP monoclonal antiserum to determine the subcellular location of the PVX replicase and TGBp2 proteins during early and late stages of virus infection. Alexa Fluor 633 conjugated secondary anti-goat sera was used to detect replicase with peak emission at 650 nm, while Alexa Fluor 488 conjugated secondary anti-mouse sera was used to detect GFP, with peak emission at 520 nm. Confocal microscopic images of at least 30 protoplasts for each time point and for each treatment were taken and replicase and GFP fusions co-localized at all time points in most cells. Fluorescence due to PVX replicase was not as abundant as fluorescence due to the GFP fusions because these proteins are expressed from different viral promoters which produce different levels of protein.

For PVX.GFP-TGBp2 at 18 hpi GFP-TGBp2 is detected mainly in vesicles or aggregates of vesicles (Figure 5A-C). At 36 hpi GFP-TGBp2 is seen in the ER as well as in vesicles (Figure 5D-F). PVX replicase is seen in vesicles at 18 and 36 h in the PVX.GFP-TGBp2 infected protoplasts. Most red vesicles seem to contain some green fluorescence at 18 hpi but more often the red and green fluorescence seems to be neighboring. These data indicate that TGBp2 and PVX replicase probably do not directly interact with each other but they are often neighboring each other. At 36 hpi the PVX replicase containing vesicles are seen along the strands of ER. These data support the notion that the PVX replicase and TGBp2 co-localize along sub-domains of the ER.

For PVX.TGBp3-GFP, green fluorescence is seen along the ER network at 12 and 48 hpi. Evidence of TGBp3-GFP in the ER network in protoplasts at early and late times following virus infection was documented by Samuels *et al*. (2007). There are some green fluorescent vesicles at 48 hpi (Figures 5G-L). Red fluorescent vesicles are seen along the ER network at 12 hpi as seen in PVX.GFP-TGBp2 infected protoplasts indicating that replicase, TGBp2, and TGBp3 likely colocalize along a sub-domain of the ER. At 48 hpi the merged image in Figure 5L shows yellow fluorescence where TGBp3 and replicase colocalize. The yellow fluorescence could indicate close association of these proteins, perhaps due to direct protein-protein interactions.

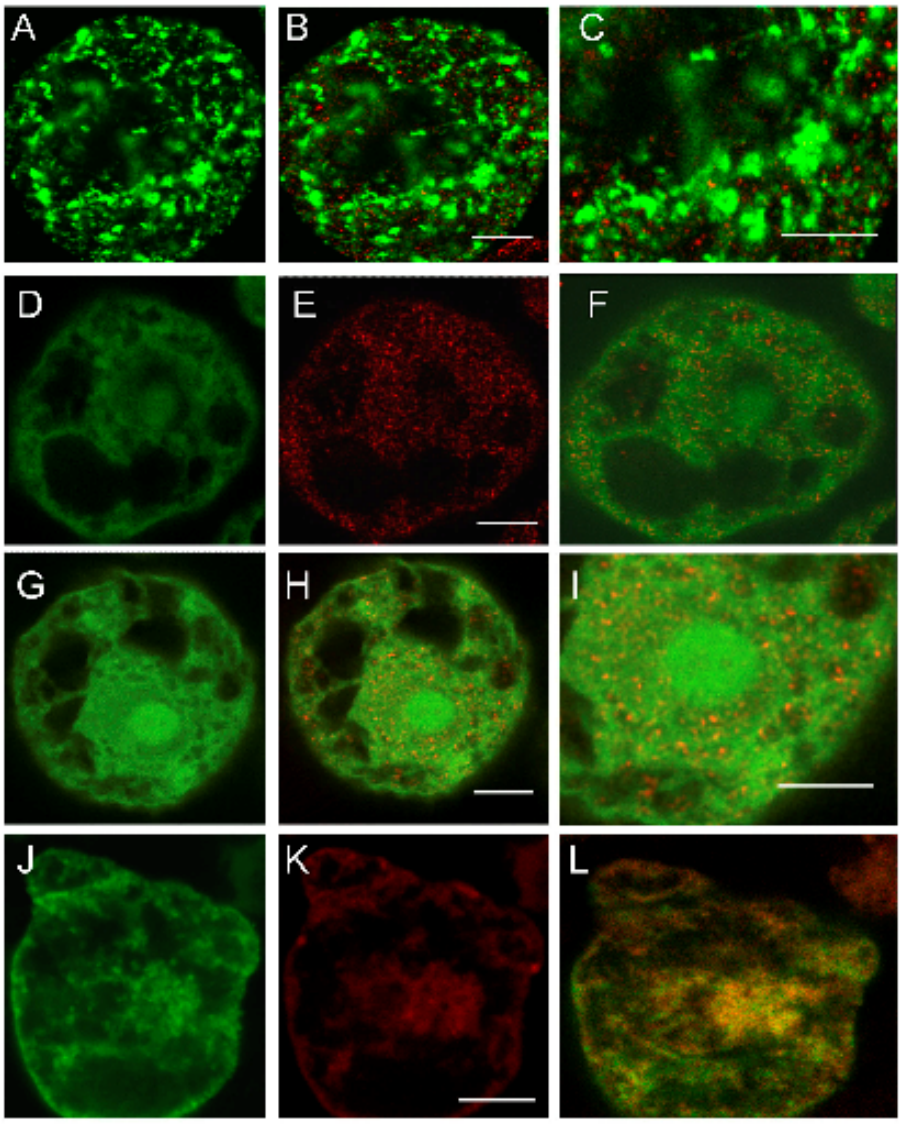
A
B
C
D
E
F
G
H
I
J
K
L

Figure 5: Confocal Images of protoplasts infected with PVX.GFP-TGBp2 and PVX.TGBp3-GFP. (A, B, C) Protoplast at 18 hpi shows green fluorescence indicating GFP-TGBp2 and red fluorescence indicating replicase. (D, E, F) Protoplast at 36 hpi shows green fluorescence indicating GFP-TGBp2 and red fluorescence indicating replicase. (G, H, I) Protoplast at 12 hpi shows green fluorescence indicating TGBp3-GFP and red fluorescence indicating replicase. (J, K, L) Protoplast at 48 hpi shows green fluorescence indicating TGBp3-GFP and red fluorescence indicating replicase. Red fluorescence indicates replicase proteins labeled with Alexa fluor 633. (C, F, I, L) The overlaid images show yellow where GFP-TGBp2 and PVX replicase or TGBp3-GFP and replicase colocalize. Bars represent 8 μm.

Imaging controls include protoplasts transfected with plasmids expressing GFP fused to an ER targeting signal (GFP-ER) were used to transfect BY-2 protoplasts. Images show the dense strands of ER extending across the vacuole from the perinuclear region toward the plasma membrane (Figure 6B). The mesh-like tubular network is not as obvious as in transfected leaf epidermal cells and this could be due to the compact size of the cells causing compression of the ER, higher prevalence of cisternae, or occurrence of perforated sheets of ER (Ridge *et al*., 1999). Protoplasts were also transfected with pRTL2-GFP-TGBp2 which shows the TGBp2 induced vesicles (Figure 6C) described in Ju *et al.*, (2005, 2007).

PVX-GFP infected protoplasts treated with replicase antiserum have green florescence in the cytoplasm and nucleus while red fluorescence is in granules scattered throughout the cytoplasm (Figure 6A). The green fluorescent granules resemble the GFP-TGBp2 induced vesicles observed in pRTL2-GFP-TGBp2 transfected protoplasts (Figure 6C).

There were mainly two patterns observed in PVX.GFP-TGBp2 inoculated protoplasts. Green fluorescence is seen in vesicles, aggregates of vesicles (Figure 6D), as well as the ER network (Figure 6E). Green and red fluorescence sometimes colocalized in vesicles and along the ER network in PVX.GFP-TGBp2 infected protoplasts that were treated with PVX replicase and Alexafluor 633 antiserum (Figure 6F-L). These data indicate that the PVX replicase can colocalize with TGBp2 in vesicles and along the ER in virus infected protoplasts, as well as in leaves.

Protoplasts transfected with pRTL2-TGBp3-GFP or infected with PVX.TGBp3-GFP show green fluorescence in the ER network (Compare figure 7A and B with 6B). PVX.TGBp3-GFP also shows fluorescence in the nucleus and perinuclear bodies which were described in Samuels et al., (2007 and Ju *et al*., In Press). When CFP-TGBp2 and TGBp3-GFP were coexpressed in protoplasts fluorescence co-localized in vesicles as seen in *N. benthamiana* leaves (compare Figure 7C-E with Figure 4D-F). PVX.TGBp3-GFP infected protoplasts were treated with replicase antisera. Green and red florescence co-localizes in vesicles and the ER network (Figure 7F-K).

The mock-inoculated samples treated with PVX replicase and Alexa fluor 633 antisera did not have evidence of green or red fluorescence (Figure 7L-N). In addition, virus infected samples treated with buffer and secondary antisera did not exhibit red fluorescence (data not shown). The combined controls indicate that green and red fluorescence are due to GFP and Alexa fluor 633 labeling of PVX replicase.

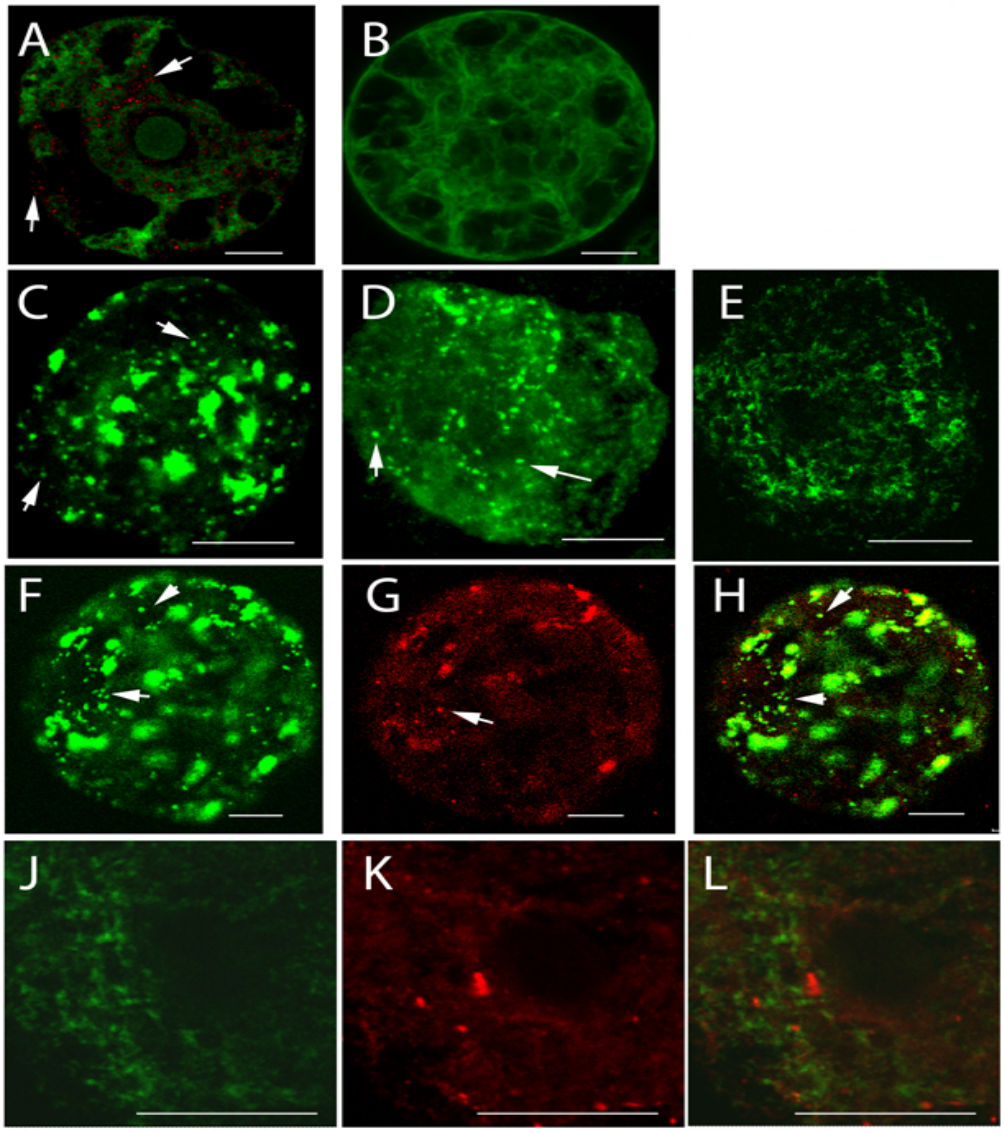
A
B
C
D
E
F
G
H
J
K
L

Figure 6. Confocal microscopic images of protoplasts transfected with viral protein -GFP fusion or infected with virus expressing viral protein -GFP fusion. Green fluorescence indicates (A) PVX-GFP, (B) GFP-ER, (C) pRTL2-GFP-TGBp2, (D, E, H, J) PVX.GFP-TGBp2. Red fluorescence indicates replicase in PVX.GFP-TGBp2 infected protoplasts (G, K). The overlaid images show yellow where GFP-TGBp2 and PVX replicase colocalize (H, L). Arrows pointed to representative examples of vesicles. Bars represent 10 μm. All images were taken using Kr/Ar laser set at 400 Hz and PMT detector within a 400 – 510 value range.

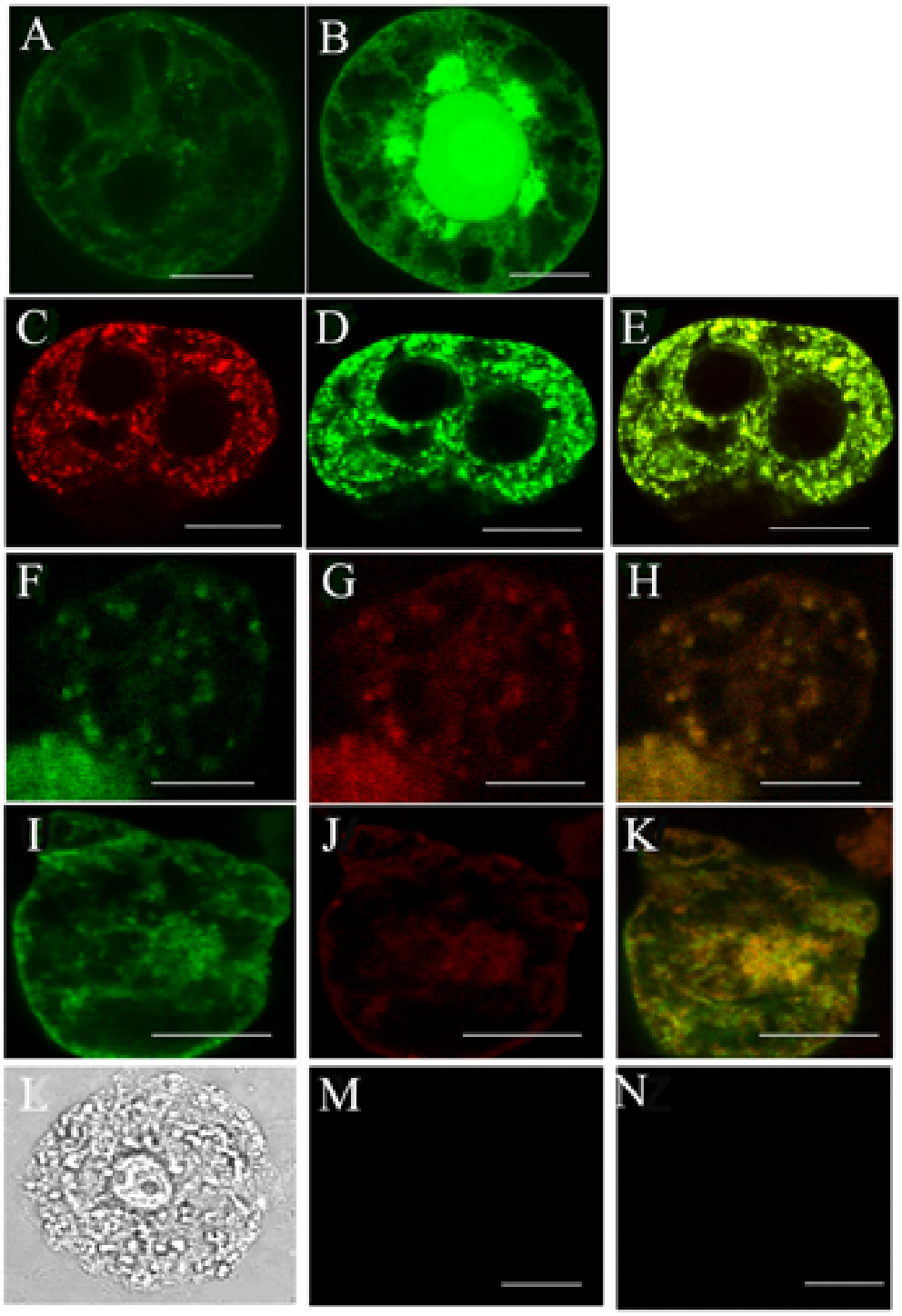
A
B
C
D
E
F
G
H
I
J
K
L
M
N

Figure 7. Confocal microscopic images of protoplasts transfected with viral protein -GFP and -CFP fusions or infected with virus expressing viral protein -GFP fusion. Green fluorescence indicates (A) pRTL2-TGBp3-GFP, (B) PVX-TGBp3-GFP, (D) pRTL2-TGBp3-GFP, (F, I) PVX-TGBp3-GFP. Red fluorescence indicates replicase in (G, J), and (C) pRTL2-CFP-TGBp2. The overlaid images show yellow where (H, K) TGBp3-GFP and PVX replicase, (E) CFP-TGBp2 and TGBp3-GFP colocalize. Panels with no signals (M, N) and transmitted image of a protoplast (L) are for mock-inoculated protoplasts labeled with PVX replicase and Alexa fluor 633 antiserum. Bars represent 10 μm. All images were taken using Kr/Ar laser set at 400 Hz and PMT detector within a 400 – 510 value range.

These data indicate that the PVX replicase co-localizes with TGBp3 in vesicles and along the ER in virus-infected protoplasts, as well as in leaves. Evidence that CFP-TGBp2 and TGBp3-GFP co-localize also further supports the hypothesis that these three proteins co-localize in vesicles and along the ER network. To determine the precise origin of these vesicles and visualize the proposed vesicles containing all three PVX proteins, further electron microscopic experiments were conducted.

Transmission electron microscopy (TEM) evaluation of the sub-cellular localization of PVX replicase, GFP-TGBp2, and TGBp3-GFP during infection in plants.

Previous reports using cryo-fixation and TEM showed GFP-TGBp2-induced novel vesicles to bud from the ER in transgenic tobacco leaves (Ju *et al*., 2005). These vesicles were co-labelled with BiP antisera. TGBp3-GFP accumulated mainly along the ER when expressed alone in transgenic leaves and no vesicles were identified which resembled those in GFP-TGBp2 expressing tissues (Ju *et al*., 2005).

In this study, PVX.TGBp3-GFP-infected and mock-inoculated tobacco leaves were cryo-fixed and embedded in either LR-White or Spurr's resin and immunogold labeling with GFP antisera, replicase antisera, or both replicase and BiP antiserum to determine the sub-cellular distribution of the TGBp3-GFP and PVX replicase proteins. Secondary antisera conjugated with 10 nm gold particles were used to detect BiP while secondary antiserum conjugated with 20 nm gold particles were used to detect GFP or PVX replicase.

If PVX replicase and TGBp3-GFP colocalize in virus infected cells, then significant quantities of immunogold label will be detected in the same sub-cellular

compartment. Since confocal microscopy experiments suggest that these proteins likely co-localize along the ER network or within ER- related vesicles, thin sections were also treated with BiP antiserum. BiP protein is an ER resident chaperone which is not present in the other areas of the endomembrane system and can be used to confirm the origin of ER-derived structures in virus infected cells (Fontes *et al*., 1991). If the PVX proteins co-localize, but in a location other than the ER, then there should be noticeable amount of immunogold label for GFP and PVX replicase in a location separate from BiP. If PVX proteins do not co-localize then there should be noticeable gold label for GFP in a location separate from gold label detecting PVX replicase. For controls, thin sections of healthy *N. benthamiana* were treated with GFP, PVX replicase, and BiP antisera. In addition, healthy and virus-infected thin sections were treated with buffer and secondary antisera.

The number of gold particles labeling specific structural components of the cell was scored in 10 μm^2 fields. Thirty five 10 μm^2 fields in which gold particles were found to be associated with cytoplasm, vacuole, cell wall (Figure 8A), chloroplast (Figure 8B), and ER (Figure 9D, E and H) were scored and the average and standard error of gold particles for all the sub-cellular structures were calculated (Table 1). Further control experiments will be added to this study before statistical analysis is to be completed by Dr. Mark Payton (Statistics Department, OSU, Stillwater, OK.).

In PVX.TGBp3-GFP infected samples treated with PVX replicase antisera, 20 nm gold particles associated mainly with strands of ER network (Figure 9D, E and H) with less labeling seen along the cell wall and cytoplasm (Table1). Table 1 shows that PVX replicase accumulation is highest in the ER in sections treated with PVX replicase

antisera or both PVX replicase and BiP antiserum. Gold particles detecting BiP are also highest in the ER, as expected. The minimal amount of gold particles (<1/10μm^2) detecting PVX replicase or BiP in the cell wall and cytoplasm is comparable to the minimal numbers of gold particles (<1/10μm^2) seen in samples treated with buffer and secondary gold conjugated sera (Table 1). Gold particles detecting PVX replicase and BiP were seen in the vacuole of virus-infected leaves. The levels of BiP seen in the vacuole of virus infected leaves was slightly higher than in healthy samples raising the possibility that PVX stimulated vacuolar targeted degradation of BiP. Pimpl *et al*. (2006) reported evidence that BiP-ligand complexes can be carried by multi vesicular bodies (MVB) to the vacuole in tobacco cells for disposal. It is worth considering that BiP may direct replicase to the vacuole for disposal after replication is completed. For GFP, the greatest amount of immunogold label was detected in the ER and lesser amounts were seen in the cytoplasm. Ju *et al*. (2008) recently demonstrated that PVX.TGBp3-GFP is degraded by the ER-associated degradation pathway (ERAD) which dislodges proteins from the ER for degradation by the 26S proteasome in the cytoplasm. Thus evidence of TGBp3-GFP in the cytoplasm is probably related to protein turnover. To conclude, these data indicate that PVX replicase, BiP, and TGBp3-GFP accumulate mainly along the ER. Antiserum detecting PVX replicase or GFP showed minimal label in the healthy samples (<1/10μm^2) indicating specific labeling of virus infected tissues.

Furthermore, specific vesicles and organelles were identified which were less abundant than the structures detailed in Table 1 and Figure 8. The numbers of gold particles labeling these specific structures were quantified, and the average and standard error of gold particles associating with each vesicle or organelle were recorded in

Table 2. The specific vesicles or organelles studied here include: protein bodies, coated vesicles (Figure 9F), ER-rich bodies (Figure 9A, B and C), mitochondria (Figure 8C), peroxisomes (Figure 8D), Golgi (Figure 9G) and plasmodesmata (Figure 8E). Since many of these structures were less abundant or rare than the structures studied in Table 1, the population numbers for each antiserum treatment vary. These vesicles and organelles were studied to further investigate whether PVX replicase or TGBp3-GFP are present in specific locations outside of the ER network.

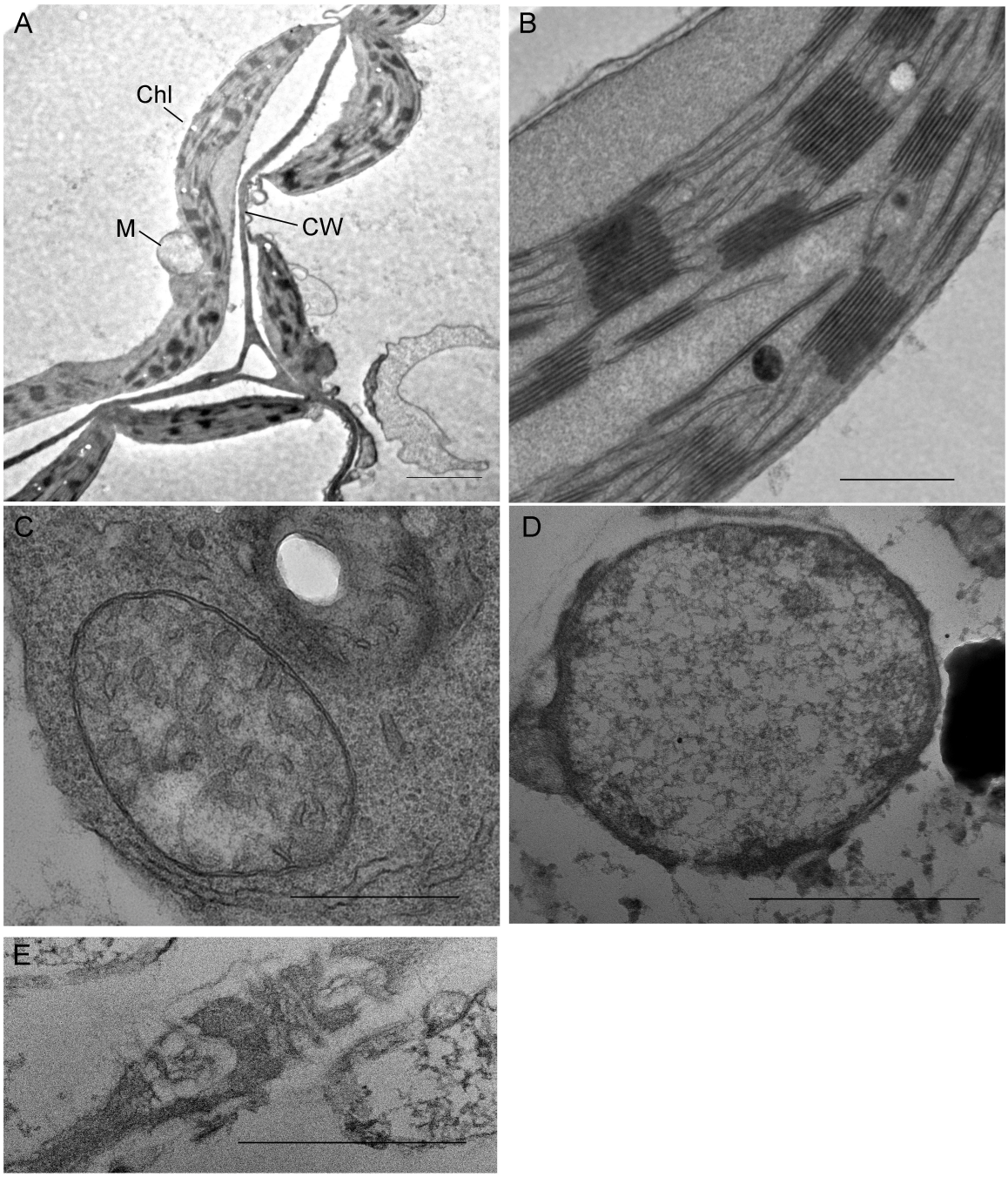
A
Chl
M
CW
B
C
D
E

Figure 8. Electron micrographs of thin sections through PVX.TGBp3-GFP inoculated leaf segments. (A) Low magnification image of a region of tissue showing neighboring cells. Chloroplast (Chl), mitochondria (M), and the cell wall (CW) are identified. (B, C, D and E) Chloroplast, mitochondria, peroxisome and plasmodesmata, respectively, treated with PVX replicase and BiP antisera. Few or no gold particles are detected in any of these organelles indicating that none of these organelles contain replicase or TGBp3-GFP. Scale bars represent 500 nm.

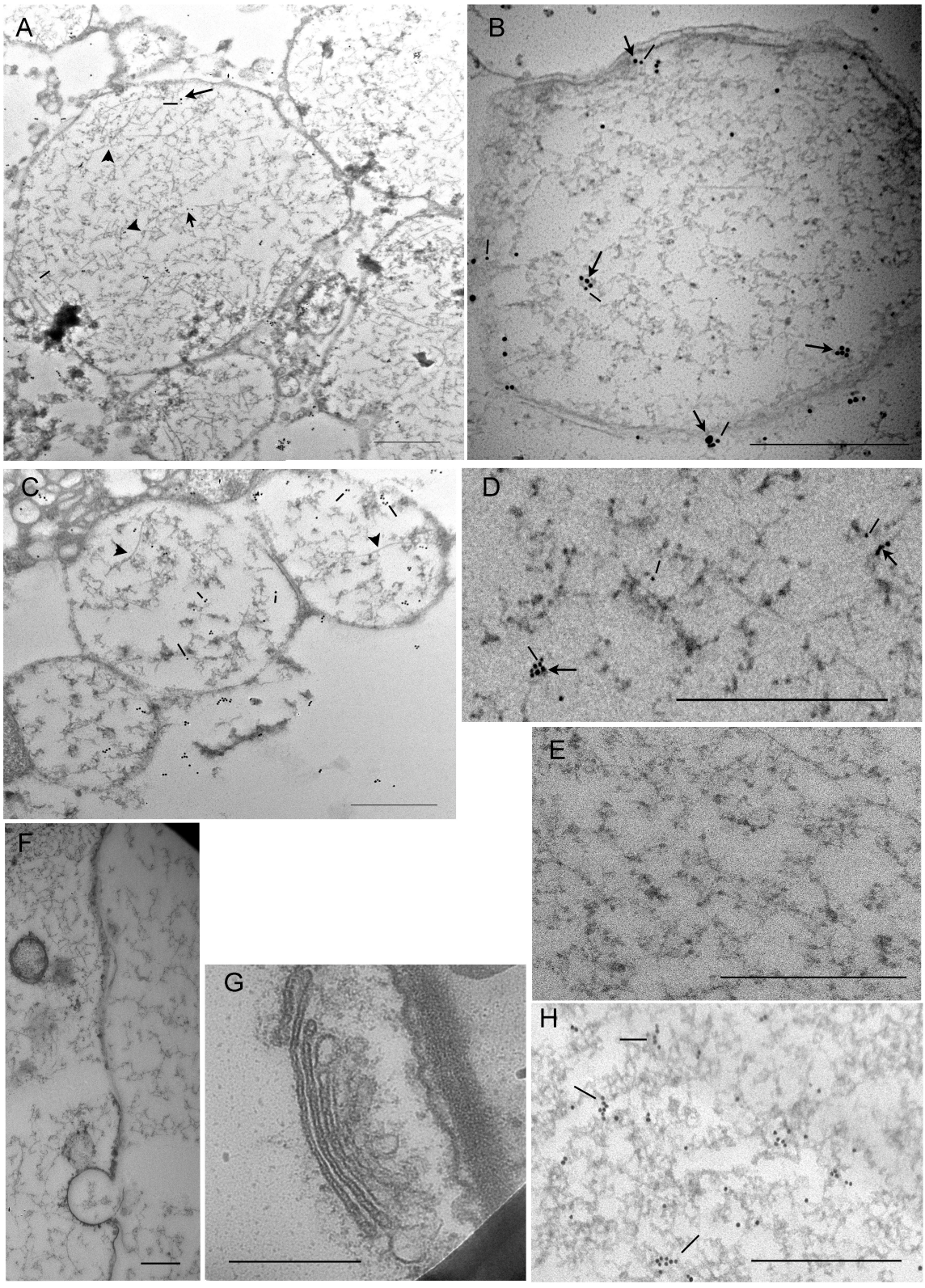
A
B
C
D
E
F
G
H

Figure 9: Electron micrographs of PVX.TGBp3-GFP and mock inoculated leaf segments. (A, B, C) ER-rich bodies found in PVX.TGBp3-GFP infected leaf tissues, but are absent from mock-inoculated leaf tissues. These are PVX-induced structures which contain virions, ER membranes, and granules which resemble ribosomes. Bodies labeled with PVX replicase, BiP, and GFP antisera. (D, E) Rough ER in PVX.TGBp3-GFP and mock-inoculated samples, treated with PVX replicase and BiP antisera, successively. (F) Image of coated vesicle budding from ER membrane. Sample was treated with PVX replicase antisera but no evidence of PVX replicase in coated vesicles. (G) Golgi apparatus in mock-inoculated sample treated with PVX replicase and BiP antisera. (H) Rough ER in PVX.TGBp3-GFP sample treated with GFP antisera. In all panels, arrowheads point to virus particles. Lines point to 10 nm gold particles which correspond to BiP antisera in all panels. Arrows point to 20 nm gold particles corresponding to PVX replicase (A, B) or GFP (C) antiserum. Scale bars represent 500 nm.

Table 1. Distribution of immunogold labeling on cell wall, cytoplasm, ER, vacuole and chloroplast with GFP, replicase, and BiP antisera in transgenic *N. benthamiana* leaves.

Sample	Treatment	# Fields	Cell Wall	Cytoplasm	ER	Vacuole	Chloroplast
PVX.TGBp3-GFP	Replicase	35	1.58±0.46	2.73±0.5	3.71±1.40	NO	NO
	Rep+BiP	35	0.57±0.10	1.00±0.17	2.40±0.41	1.31±0.30	0.00±0.00
	Rep+BiP	35	0.86+0.14	0.31±0.05	4.43±0.75	3.43±0.75	0.29±0.05
	buffer	35	0.10±0.02	0.54±0.09	0.06±0.01	0.44±0.19	NO
	GFP	35	0.43±0.08	0.97±0.16	2.80±0.47	0.00±0.00	NO
Healthy							
	Rep+BiP	35	0.00±0.00	0.00±0.00	0.14±0.02	0.13+0.04	0.00±0.00
	Rep+BiP	32	0.03±0.01	0.00±0.00	2.57±0.43	2.13±0.75	0.32±0.06
	buffer	NO	NO	NO	NO	NO	NO
	GFP	35	0.36±0.10	0.10±0.02	0.11±0.02	0.00±0.00	NO

PVX.TGBp3-GFP infected *N. benthamiana* leaf segments were embedded in LR White, sectioned, and analyzed by immunogold labeling and electron microscopy to assess the sub-cellular accumulation patterns of TGBp3-GFP and replicase. Control samples included noninoculated healthy leaves. Immunogold labeling was conducted using commercially available full-length mouse monoclonal AV antiserum (BD living colors; CLONTECH Laboratories) to detect GFP, BiP rabbit antiserum (Affinity BioReagents), PVX replicase goat antisera obtained from Cindy Hemenway (NC State University), or no primary antiserum (buffer). Samples were treated with 10 nm gold-conjugated anti-mouse to detect GFP. Samples were dual-labeled using antiserum to detect replicase and BiP and were treated with 20 nm and 10 nm of gold-conjugated anti-goat and anti-rabbit sera (specific particles counted in dual labeling experiments noted with red labeling). Fields are defined as areas of 10 μm^2 (using an ultrastructure size calculator) that contain gold particles. Gold particles in each field were counted manually, average and standard error was calculated and, tabulated. The total numbers of fields analyzed for each plant sample are indicated. The numbers of gold particles detected in the cell wall (CW), cytoplasm, ER, vacuole, and chloroplast were determined for all fields treated with each antiserum. Zeros indicate sub-cellular domains with no label. NO indicates that the structure was not observed.

In PVX.TGBp3-GFP infected samples, I found two virus-induced novel structures: coated vesicles and ER-derived vesicles. The coated vesicles appear to form from rough endoplasmic reticulum (RER) and the average diameter determined from 21 vesicles is 375.95 $\pm$82.04 nm (Figure 9F). These vesicles appear to be coated with dense granules and were undetected in healthy *N. benthamiana* sections. The coated vesicles had low levels of gold label, detection of PVX replicase or BiP and, there was no label detecting GFP (Table 2). These coated vesicles may be fewer in healthy cells, and therefore not easily found, or represent pathological structures unrelated to replication or virus movement. It is possible that PVX infections causes an increase in the numbers of COPII or COPI coated vesicles compared to the non-infected samples making them easier to detect. Other ER-derived vesicles were found in virus-infected but not healthy leaf sections (Table 2). These ER-derived vesicles are larger, having an average diameter determined from 21 vesicles to be 1048.14 $\pm$228.72 nm (Figure 9A-C). These vesicles contain virus particles and ribosomes, and membraneous strands which label with PVX replicase, GFP, and BiP antisera. The PVX TGBp2 related ER-derived vesicles described in Ju *et al*., (2005) were 150-500 nm in diameter and similarly labeled with ribosomes and BiP. It is possible that the larger ER-derived vesicles seen in PVX infected samples have the same origin as the TGBp2 related vesicles described previously. It is worth speculating that these vesicles induced by TGBp2 become larger, as caused by events during virus infection, to contain virions and replicating virus.

In PVX.TGBp3-GFP infected samples, immunolabeling detected PVX replicase, BiP and GFP mainly in ER-derived vesicles (Table 2) and minimal label was found to be associated with protein bodies, coated vesicles, mitochondria, peroxisomes, Golgi and

plasmodesmata. Surprisingly, Golgi stacks were not easily identified in PVX.TGBp3-GFP infected samples compared to healthy samples. This may be evidence Golgi stacks are depleted during virus infection, or that there were similar difficulties in detecting Golgi as for detecting coated vesicles in healthy samples. Healthy samples had minimal labeling with GFP, RdRp, and BiP antisera.

Table 2. Distribution of immunogold labeling on protein bodies, coated vesicles, ER-rich bodies, mitochondria, peroxisomes, Golgi and plasmodesmata, with GFP, replicase, and BiP antisera in transgenic *N. benthamiana* leaves.

Sample or Treatment	Fields	Protein Bodies	Coated Vesicles	ER-rich Bodies	Mito-chondria	Peroxi-somes	Golgi	Plasmo-desmata
PVX.TGBp3-GFP								
Replicase	6 to 13	NO	NO	7.77±2.15	NO	0.67±0.22	NO	NO
Replicase+BiP	6 to 35	0.00±0.00	0.70±0.12	3.10±0.58	0.00±0.00	0.00±0.00	0.00±0.00	0.00±0.00
Replicase+BiP	6 to 35	0.00±0.00	0.80±0.14	6.17±1.15	0.09±0.02	0.20±0.03	0.00±0.00	0.00±0.00
buffer	NO	NO	NO	NO	NO	NO	NO	0.00±0.00
GFP	20-29	NO	0.08±0.02	1.90±0.42	NO	0.07±0.01	NO	NO
Healthy								
Replicase+BiP	27 to 35	0.00±0.00	NO	NO	0.09±0.01	0.00±0.00	0.00±0.00	NO
Replicase+BiP	27 to 35	0.00±0.00	NO	NO	0.09±0.01	0.17+0.00	0.00±0.00	NO
buffer	NO	NO	NO	NO	NO	NO	NO	NO
GFP	17	NO	NO	NO	NO	0.00+0.00	NO	NO

PVX.TGBp3-GFP infected and mock (Healthy) inoculated *N. benthamiana* leaf segments were embedded in LR White, sectioned, and analyzed by immunogold labeling and electron microscopy to assess the subcellular accumulation patterns of TGBp3-GFP and replicase. Control samples included noninoculated healthy leaves. Immunogold labeling was conducted using commercially available full-length mouse monoclonal GFP antiserum (BD living colors; CLONTECH Laboratories), BiP rabbit antiserum (Affinity BioReagents), PVX replicase goat antisera obtained from Cindy Hemenway (NC State University), or no primary antiserum (buffer). Samples were treated with 10 nm gold-conjugated anti-mouse to detect GFP. Samples were dual-labeled using antiserum to detect replicase and BiP and were treated with 20 nm and 10 nm of gold-conjugated anti-goat and anti-rabbit sera (specific particles counted in dual labeling experiments noted with red labeling). Fields are defined as each organelle that contains gold particles. Gold particles in each organelle were counted manually, average and standard error was calculated and, tabulated. The total numbers of organelles analyzed for each plant sample are indicated. The numbers of gold particles detected in protein bodies, coated vesicles, ER-rich bodies, mitochondria, peroxisomes, Golgi and plasmodesmata were determined for all fields treated with each antiserum. Zeros indicate subcellular domains with no label. NO indicates the structures were not observed.

In combination, immunofluorescence and immunogold labeling detected TGBp3-GFP and replicase co-localize along the ER network and ER-derived vesicles. These novel ER-derived vesicles identified by electron microscopy contain virus particles, TGBp3-GFP protein and replicase protein. Considering the time-lapse imaging for TMV which shows that the TMV movement and movement associated proteins carry membrane associated replication complexes toward plasmodesmata (Asurmendi *et al*., 2004; Kawakami *et al*., 2004, and Liu *et al*., 2005), it is possible that TGBp2 and TGBp3 proteins traffic replicating PVX virus and virions toward plasmodesmata in these ER-derived vesicles.

Sucrose gradient fraction of PVX.TGBp3-GFP infected tobacco leaves.

Sucrose gradient fractionation was used to determine if the ER-derived structures containing PVX replicase and TGBp3-GFP could be separated from other components of the endomembrane network. Fractions were subjected to immunoblot analysis to determine if the PVX replicase, TGBp3-GFP and BiP co-fractionate as predicted based on confocal and electron microscopic experiments. Fractions were also treated with antisera recognizing other subdomains of the secretory system. The antisera tested recognize: PVX replicase, GFP, BiP (an ER resident protein used as a marker to identify fractions containing ER membranes), SYP21 (which resides in the late endosome and vacuole) SYP41 (which resides in the trans Golgi network [TGN]) and SYP61 (which resides in the TGN and endosome). All SYP antiserum were obtained from Dr. Tony Sanderfoot at University of Minnesota (Bar- Peled and Raikhel 1997; Sanderfoot *et al.*, 1999; Bassham *et al.*, 2000).

Protein extracts from PVX.TGBp3-GFP infected and mock-inoculated *N. benthamiana* leaves were loaded onto 20-60 % continuous sucrose gradients. Sixteen 0.5 ml-fractions were collected from the top of the gradient, leaving behind the chlorophyll fraction at the bottom. Proteins were concentrated and run on an SDS polyacrylamide gel and transferred to nitrocellulose for immunoblot analysis. Since the replicase antisera recognize intact and not denatured proteins, fractions were also loaded onto slot blots and then treated with PVX replicase antisera.

PVX.TGBp3-GFP infected *N. benthamiana* leaf extracts treated with GFP antisera show bands mainly in the first five fractions. As expected GFP was not detected in fractions of healthy leaf extracts (Figure 10). Fractions 1-5 of PVX.TGBp3-GFP infected leaf extracts tested positive for replicase and BiP indicating that these three proteins colocalize in ER membranes.

SYP21, SYP41, and SYP61 antisera were used to characterize the distribution of the trans Golgi network, endosome, and vacuolar membranes across the sucrose gradient. These proteins were not detected in fractions 1-5 but were distributed across fractions 6-16. These data show a clear separation of the ER resident proteins from later components of the endomembrane network providing clearer evidence that the PVX replicase and TGBp3 do not associate with the Golgi or post-Golgi networks. Interestingly, the band intensity for SYP41, and SYP61 proteins were greater in virus infected than healthy samples suggesting that PVX infection may have caused upregulation of these secretory proteins.

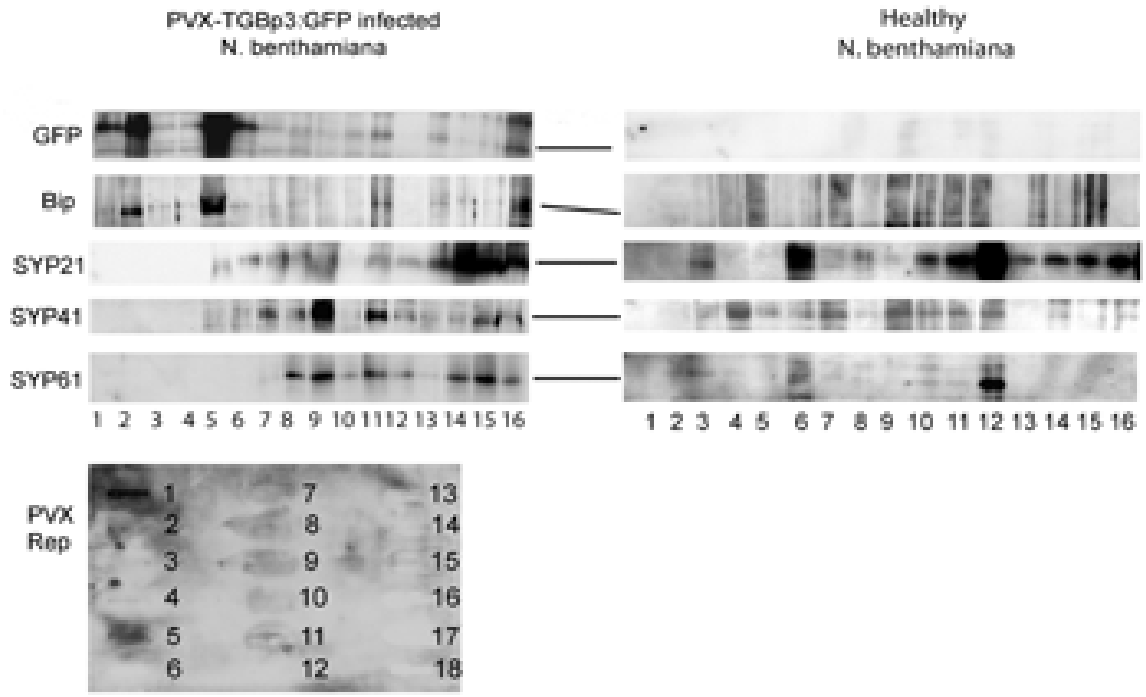

Figure 10: Sucrose gradient analysis for viral replicase, TGBp3-GFP, and host proteins representing various membraneous fractions. Extracts from PVX.TGBp3-GFP infected and healthy *N. benthamiana* plants were fractionated on a sucrose gradient and fractions were subjected immunoblot analysis using PVX replicase, GFP, BiP, SYP21, SYP41 and SYP 61 antisera. Fractions 1 to 16 of PVX.TGBp3-GFP infected and healthy leaf extracts appear in each membrane. Slot blot analysis with PVX.TGBp3-GFP protein extract treated with replicase antisera is also shown.

Densitometry was used to study changes in band intensities across the auto-radiographs for each immunoblot and to compare protein distributions in fractions of PVX.TGBp3-GFP infected and healthy leaf protein extracts. The final values are presented as relative density values (RDV) (Figure 11).

Relative densitometry values for PVX.TGBp3-GFP infected protein extracts show 34- or 36-fold more TGBp3-GFP or replicase than in protein extracts from healthy tissue (Figure 11A and B). BiP was detected mainly in fractions 1-5 in infected tissues (Figure 11C). BiP was also detected in the same fractions as SYP21 (which is in the vacuole). This data support earlier described electron microscopic studies which found noticeable amount of BiP in the vacuole of virus-infected cells.

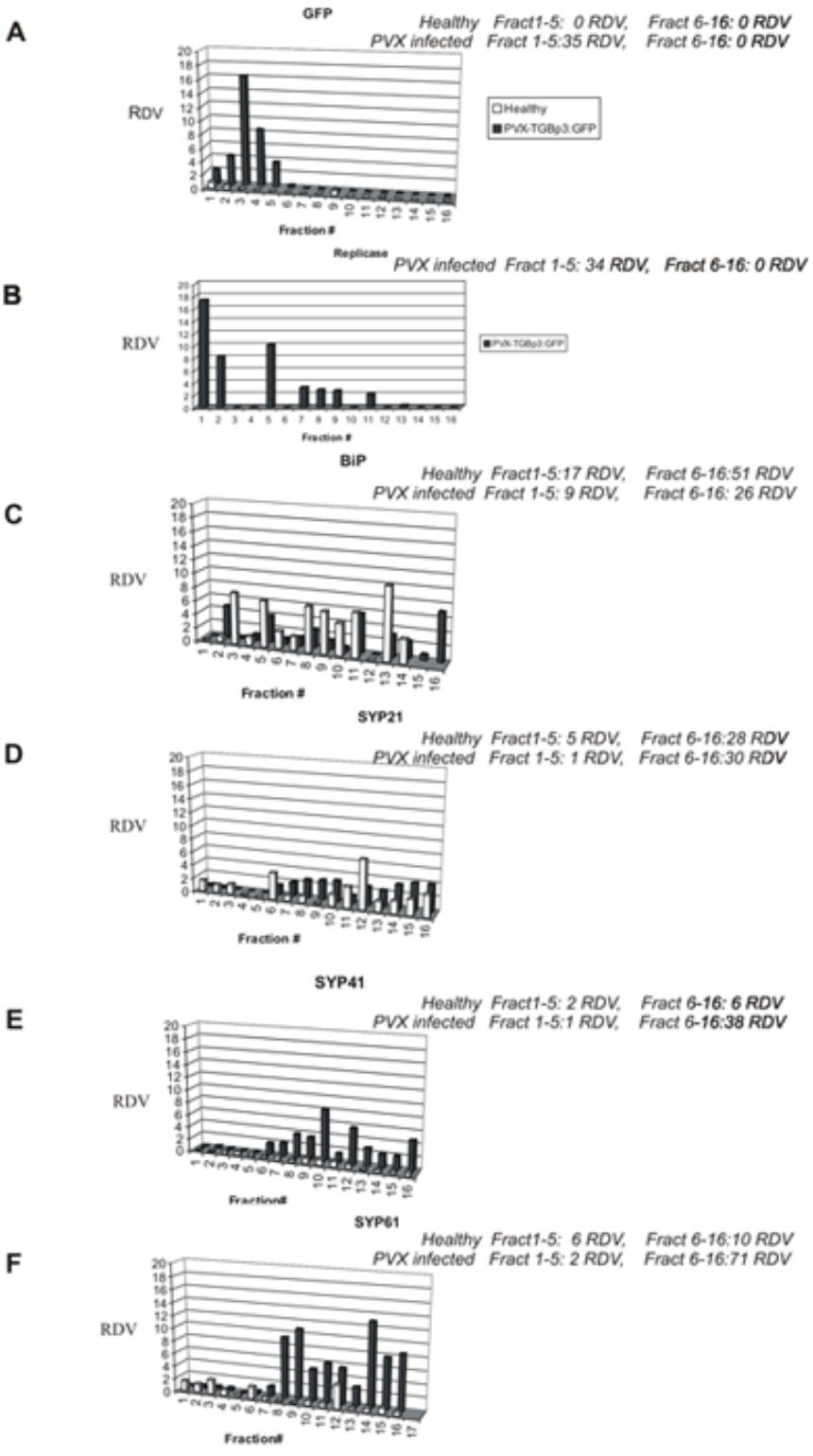
A
GFP
Healthy Fract1-5: 0 RDV, Fract 6-16: 0 RDV
PVX infected Fract 1-5:35 RDV, Fract 6-16: 0 RDV
RDV
Healthy
PVX-TGBp3:GFP
Fraction #
B
Replicase
PVX infected Fract 1-5: 34 RDV, Fract 6-16: 0 RDV
RDV
PVX-TGBp3:GFP
Fraction #
C
BiP
Healthy Fract1-5:17 RDV, Fract 6-16:51 RDV
PVX infected Fract 1-5: 9 RDV, Fract 6-16: 26 RDV
RDV
Fraction #
D
SYP21
Healthy Fract1-5: 5 RDV, Fract 6-16:28 RDV
PVX infected Fract 1-5: 1 RDV, Fract 6-16:30 RDV
RDV
Fraction #
E
SYP41
Healthy Fract1-5: 2 RDV, Fract 6-16: 6 RDV
PVX infected Fract 1-5:1 RDV, Fract 6-16:38 RDV
RDV
Fraction#
F
SYP61
Healthy Fract1-5: 6 RDV, Fract 6-16:10 RDV
PVX infected Fract 1-5: 2 RDV, Fract 6-16:71 RDV
RDV
Fraction#

Figure 11: Density gradient analyses of the distribution of sub-cellular membranes of PVX.TGBp3-GFP infected and healthy *N. benthamiana* leaves. Immunoblot assays were performed to identify GFP, BiP, SYP 21,SYP 41, SYP 61 and replicase proteins. Fraction number was plotted against relative density value.

CHAPTER V

CONCLUSION AND DISCUSSION

The replication of positive-sense RNA viruses is typically associated with cellular membranes and there are many examples of viruses which induce invaginations of cellular membranes to protect the replicating virus from host defenses (Restrepo-Hartwig and Ahlquist, 1996; Heinlein *et al.,* 1998; Reichel and Beachy, 1998; Russo *et al.*, 1983; Lupo *et al.*, 1994; Schwartz *et al.,* 2002; Schwartz *et al.,* 2004). In this study, we used confocal microscopy, transmission electron microscopy, and sucrose gradient fractionation followed by immunoblot analysis to detect the subcellular localization of the PVX replicase and to determine if PVX TGBp2 and TGBp3 reside in the same subcellular domain. Confocal microscopic analysis of leaves indicated that all infected epidermal and mesophyll cells contain replicase, GFP-TGBp2, and TGBp3-GFP along the ER network and ER-derived vesicles, while results from infected protoplasts indicated that the PVX replicase co-localizes with TGBp3 in vesicles and along the ER. Evidence that CFP-TGBp2 and TGBp3-GFP colocalize also further supports the hypothesis that these three PVX proteins colocalize in vesicles and along the ER network.

Time course experiments in protoplasts found no evidence that the co-localization of PVX replicase, GFP-TGBp2 or TGBp3-GFP varies with time. Proteins were found to co-localize in vesicles and along the ER in cells early and late in infection. Immunofluorescence labeling with PDI antisera and immunogold labeling with BiP

antisera confirmed that these three PVX proteins co-localize along ER strands and in ER-derived vesicles.

Prior literature has stated that PVX replicase associates with cellular membranes (Doronin and Hemenway, 1996; Plante *et al*., 2000), but no work was done to identify the type of membrane compartment where PVX replicates. Considering reports that BMV replication occurs in invaginations protruding into the ER lumen along with reports that poliovirus replication occurs in novel vesicles derives from ER (Schwartz *et al*., 2002, 2004; Schlegel *et al.*, 1996; Suhy *et al*. 2000), we undertook this study to determine if PVX replicase colocalizes with TGBp2 and TGBp3 proteins which are known to reside in the ER and ER-derived vesicles.

Virus-infected and mock-inoculated leaf segments were harvested at 5 dpi and subjected to both cryo-fixation and embedding in LR-White or, chemical fixation and embedding in Spurr's resin for transmission electron microscopic studies. The two methods of tissue preparation have different benefits. Cryo-fixation is superior for preservation of antigenicity of cytosolic proteins and is comparable to chemical fixation for preservation of membrane structures (Howard, 2001). Chemical fixation is superior for preservation of certain cellular structures, although antigenic structures in plants that are sensitive to aldehyde are negatively impacted by the fixative and by the time for fixation relative to the more rapid cryo-fixation method (Ripper *et al*., 2007). Spurr's resin and LR-White were both used in case the nature of the embedding resin might impact tissue preservation and staining.

Electron microscopic studies identified novel ER-derived vesicles containing PVX replicase, TGBp3-GFP, and virions. Virion particles are around 500 nm in length

and easily cargo in the 1048.14 ±228.72 nm novel ER –derived vesicles (Figure 9A, B and C). These vesicles were not found in healthy plant tissues suggesting that they are virus-induced structures. Electron microscopic experiments are under way to find out whether TGBp2 protein is also present in these vesicles. Time-lapse imaging for TMV shows that the TMV movement and movement-associated proteins carry membrane associated replication complexes which has replicase, MP, CP, and viral RNA toward plasmodesmata (Asurmendi *et al*., 2004; Kawakami *et al*., 2004 and Liu *et al*., 2005). Probably these PVX induced vesicles also function to transport viral nucleic acids and proteins to the plasmodesmata.

Electron microscopic analysis of PVX.TGBp3-GFP infected leaf segments found a second class of vesicles which appear to be coated with dense granules, here called coated vesicles (Figure 9F). These vesicles are 375.95 ±82.04 nm in diameter, which is smaller than the length of a virus particle. These vesicles show low levels of immunogold labeling detecting PVX replicase, BiP, or GFP (Table 2) suggesting that these structures are unrelated to PVX replication or movement. Further analysis is needed to clarify the role (if any) of these vesicles in virus infection.

Fractionation and densitometry analyses identified PVX replicase, TGBp3-GFP, and BiP in the first five fractions near the top of the gradient, providing further support that these PVX proteins target to the ER or ER-derived vesicles. SYP41 and SYP61 localize to the trans Golgi network and endosome, and there is a total 4-5 fold increase in these proteins in PVX infected fractions over healthy fractions. SYP21, SYP41, and SYP61 are not detected in the same fractions as PVX replicase, TGBp3, and BiP

indicating that these PVX proteins do not traffic through the secretory system but more often reside in the ER.

Interestingly, we detected BiP and PVX replicase in the vacuolar lumen of virus infected leaves by immunogold labeling and electron microscopy. SYP21 localizes to the endosomal and vacuolar membrane and failed to co-localize with BiP and replicase in sucrose gradient fractions. These data demonstrate that PVX replicase and BiP do not accumulate along the vacuolar membrane but do not preclude vacuolar degradation of these proteins. Previous reports have shown that BiP is exported from the ER via a pathway involving COPII vesicles and multivesicular bodies (Pimpl *et al*., 2003; 2006; daSilva *et al*., 2005) to the vacuole (Tse *et al*., 2004; Sanderfoot *et al*., 1998). Since we failed to detect adequate Golgi stacks, COPII vesicles, or multivesicular bodies in this study we can only speculate that PVX replicase follows the same route as BiP to the vacuole for degradation. Further experiments are needed to determine the path for degradation of the PVX replicase.

Studies have shown that the PVX TGBp2 and TGBp3 are exported from the ER to the cytosol for degradation. Recently Ju *et al*. (2008) showed PVX TGBp3-GFP also traffics into the nucleus. General accumulation of TGBp3-GFP is impacted by inhibitors of the 26S proteasome suggesting that these proteins are degraded by the ERAD pathway. Thus the pathway for degradation of the PVX replicase is likely to be distinct from TGBp2 and TGBp3.

Combining the results of this study with those of Ju *et al*. (2005, 2008), I propose a new model to describe PVX replication, cell-to-cell spread, and protein turnover. First, PVX replicase, TGBp2, and TGBp3 colocalize along the ER or ER-derived vesicles.

These vesicles contain PVX virions, replicase, TGBp2 and TGBp3. We propose that the vesicles carry infectious agents and viral movement proteins to the plasmodesmata for transport into neighboring cells. The 1 μm diameter vesicles observed in this study appear like larger versions of the GFP-TGBp2 150- 500 nm diameter vesicles reported by Ju *et al*. (2005). Both vesicles co-label with antisera detecting TGBp3-GFP and BiP and appear early in infection, as seen in protoplasts. Further electron microscopic and sucrose gradient fractionation need to be conducted to determine if GFP-TGBp2 co-localizes in the replicase containing vesicles or in another vesicle population. The result presented in this study and in related studies indicates that PVX replicase, GFP-TGBp2 (Ju *et al*., 2005, 2007) or TGBp3-GFP proteins were found to colocalize in ER-derived vesicles and along the ER in cells early and late in infection. The results here resemble results reported for TMV showing that the viral replicase along with the movement and movement associated proteins carries infectious agents to the plasmodesmata in membrane associated complexes (Asurmendi *et al*., 2004; Kawakami *et al*., 2004 and Liu *et al*., 2005). Considering the model proposed for TMV movement, it is possible that PVX replication complexes are also transported to the plasmodesmata by a similar mechanism (Figure 12).

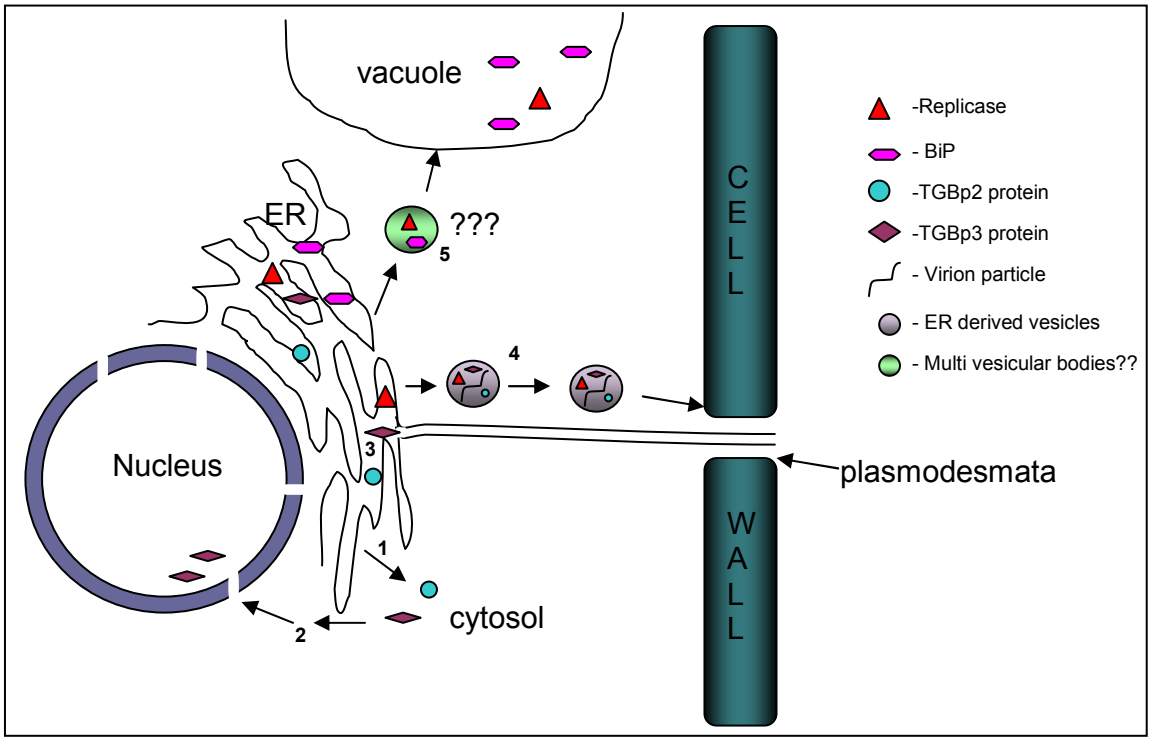

Figure 12: Model describing PVX replication, cell-to-cell spread, and protein turnover. (1) PVX TGBp2 and TGBp3 export from the ER to the cytosol for degradation. (2) PVX TGBp3-GFP traffics into the nucleus. (3) PVX replicase, TGBp2, and TGBp3 colocalize along the ER or ER-derived vesicles. (4) ER-derived vesicles carry infectious agents and viral movement proteins to the plasmodesmata for transport into neighboring cells. (5) Replicase and BiP export from the ER via a pathway involving COPII vesicles and multivesicular bodies to the vacuole.

REFERENCES

Angell, S. M., Davies, C., and Baulcombe, D. C. (1996). Cell-to-cell movement of *Potato virus X* is associated with a change in the size-exclusion limit of plasmodesmata in trichome cells of *Nicotiana clevelandii*. *Virology* **216**, 197-201.

Appiano, A., Bassi, M., and D'Agostino, G. (1983). Cytochemical and auto radiographic observations on tomato bushy stunt virus- induced multivesicular bodies. *Ultramicroscopy* **12,** 162.

Appiano, A., D'Agostino, G., Bassi, M., Barbieri, N., Viale, G. and Dell'Orto, P. (1986). Origin and function of tomato bushy stunt virus-induced inclusion bodies. 11. Quantitative electron microscope autoradiography and immunogold cytochemistry. *J Ultrastruct Mol Struct Res* **97,** 31-38.

Asurmendi, S., Berg, R. H., Koo, J. C. and Beachy, R. N. (2004). Coat protein regulates formation of replication complexes during tobacco mosaic virus infection. *Proc Natl Acad Sci* **101**, 1415–1420.

Bancroft, J. B., Rouleau, M., Johnston, R., Prins, L. and Mackie, G.A. (1991). The entire nucleotide sequence of foxtail mosaic virus RNA. *J Gen Virol* **72,** 2173–2181.

Bar-Peled, M. and Raikhel, N.V. (1997). An Efficient Method for Cloning In-Frame Fusion Protein Genes. *Anal Biol* **250**, 262-264.

Bassham, D. C., Sanderfoot, A.A., Kovaleva, V., Zheng, H. and Raikhel, N.V. (2000). AtVPS45 complex formation at the trans-Golgi network. *Mol Biol Cell* **11**, 2251-2265.

Batten, J. S., Yoshinari, S. and Hemenway, C. (2003). Potato virus X; a model system for virus replication, movement and gene expression. *Mol Plant Pathol* **4(2),** 125-131.

Baulcombe (1995). Jellyfish green fluorescent protein as a reporter for virus infections. *Plant J* **7,** 1045–1053.

Beck (1991). Triple gene block proteins of white clover mosaic potexvirus are required for transport. *Virology* **183,** 695-702.

Buck (1996). Comparison of the replication of positive-stranded RNA viruses of plants and animals. *Adv Virus Res* **47,** 159–251.

Carette, J. E., Stuiver, M., Van Lent, J., Wellink, J. and van Kammen, A. (2000). Cowpea mosaic virus infection induces a massive proliferation of endoplasmic reticulum but not golgi membranes and is dependent on *de novo* membrane synthesis. *J Virol* **74,** 6556-6563.

daSilva, L. L., Taylor, J.P., Hadlington, J.L., Hanton, S.L., Snowden,C.J., Fox, S.J., Foresti, O., Brandizzi, F., and Denecke, J. (2005). Receptor salvage from the prevacuolar compartment is essential for efficient vacuolar protein targeting. *Plant Cell* **17**, 132–148.

Davenport, G. F. and Baulcombe, D.C. (1997). Mutation of the GKS motif of the RNA-dependent RNA polymerase from potato virus X disables or eliminates virus replication. *J Gen Virol* **78,** 1247–1251.

de Graaf, M., Coscoy, L. and Jaspars, E.M.J. (1993). Localization and biochemical characterization of alfalfa mosaic virus replication complexes. *Virology* **194,** 878-881.

Demler, S. A., Borkhsenious, O.N., Rucker, D.G. and de Zoeten, G.A. (1994). Assessment of the autonomy of replicative and structural functions encoded by the Luteo-phase of pea enation mosaic virus. *J Gen Virol* **75,** 997-1007.

Doronin, S. V. and Hemenway, C. (1996). Synthesis of potato virus X RNAs by membrane-containing extracts. *J Virol* **70**, 4795–4799.

Dunoyer, P., Ritzenthaler, C., Hemmer,O., Michler,P. and Fritsch, C. (2002). Intracellular Localization of the Peanut Clump Virus Replication Complex in Tobacco BY-2 Protoplasts Containing Green Fluorescent Protein-Labeled Endoplasmic Reticulum or Golgi Apparatus. *J Virol* **76; 2**, 865-874.

Fontes, E. B. P., Shank, B. B., Wrobel, R. L., Moose, S. P., OBrian, G. R., Wurtzel, E. T. and Boston, R. S. (1991). Characterization of an Immunoglobulin Binding Protein Homolog in the Maize floury-2 Endosperm Mutant. *Plant cell* **3**, 483-496.

Garnier, M., Candresse, T. and Bové, J.M. (1986). Immunocytochemical localization of TYMV coded structural and non-structural proteins by the protein A-gold technique. *Virology* **151**, 100-109.

Goregaoker, S. P., Lewandowski, D.J. and Culver, J.N. (2001). Oligomerization and activity of the helicase domain of the tobacco mosaic virus 126- and 183-kilodalton replicase proteins. *J Virol* **77,** 3549-3556.

Harrison, B.D. and Roberts, I.M. (1968). Association of tobacco rattle virus with mitochondria. *J Gen Virol* **3,** 121-124.

Haseloff, J., Siemering, K.R., Prasher, D.C. and Hodge, S., (1997). Removal of a cryptic intron and subcellular localization of green fluorescent protein are required to mark transgenic *Arabidopsis* plants brightly. *Proc Natl Acad Sci* **94**, 2122–2127.

Hatta, T. and Francki, R.I.B. (1981). Cytopathic structures associated with tonoplasts of plant cells infected with cucumber mosaic and tomato aspermy viruses. *J Gen Virol* **53,** 343-346.

Heinlein, M., Padgett, H.S. and Gens, J.S. (1998). Changing patterns of localization of TMV movement protein and replicase to endoplasmic reticulum and microtubules during infection. *Plant Cell* **10,** 1107-1120.

Howard, R. J. (2001). Cytology of fungal pathogens and plant—host interactions *Curr Opinion Microbiol* **4**, 365-373

Howard, A. R., Heppler, M. L., Ju, H.-J., Krishnamurthy, K., Payton, M. E., and Verchot-Lubicz, J. (2004). *Potato virus X* TGBp1 induces plasmodesmata gating and moves between cells in several host species whereas CP moves only in *Nicotiana benthamiana* leaves. *Virology* **328**,185-197.

Huisman, M. J., Linthorst, H. J. M., Bol, J. F. and Cornelissen, B. J. C. (1988). The complete nucleotide sequence of Potato virus X and its homologies at the amino acid level with various plus-stranded RNA viruses. *J Gen Virol* **69,** 1789–1798.

Ju, H.-J., Samuels, T.D., Wang, Y.S., Blancaflor, E., Payton, M., Mitra, R., Krishnamurthy, K., Nelson, R.S. and Verchot-Lubicz, J. (2005). The potato virus X TGBp2 movement protein associates with endoplasmic reticulum-derived vesicles during virus infection. *Plant Physiol* **138,** 1877-1895.

Ju, H. J., Brown, J., Ye, C.M, Verchot-Lubicz, J. (2007). Mutations in the central domain of potato virus X TGBp2 eliminate granular vesicles and virus cell-to-cell trafficking. *J Virol* **81**, 1899-1911.

Ju, H. J., Ye, C.M. and Verchot-Lubicz, J. (2008). Mutational analysis of PVX TGBp3 links subcellular accumulation and protein turnover. *Virology* **in press**.

Kawakami, S., Watanabe, Y., Beachy, R.N. (2004). Tobacco mosaic virus infection spreads cell to cell as intact replication complexes. *PNAS* **101,** 6291-6296.

Kim, K. H., Kwon, S.J. and Hemenway, C. (2002). Cellular protein binds to sequences near the 5'-terminus of potato virus X RNA that are important for virus replication. *Virology,* **301,** 305–312.

Kim, K. H. a. H., C. (1996). The 5' nontranslated region of potato virus X RNA affects both genomic and sub genomic RNA synthesis. *J Virol* **70,** 5533-5540.

Kiss, J. Z., Giddings, T.H. Jr., Staehelin, L.A. and Sack, F.D. (1990). Comparison of the ultrastructure of conventionally fixed and high pressure frozen/freeze substituted root tips of Nicotiana and Arabidopsis. *Protoplasma* **157**, 64-74.

Koonin, E. V. a. D., V.V. (1993). Evolution and taxonomy of positive-strand RNA viruses: implications of comparative analysis of amino acid sequences. *Crit Rev Biochem Mol Biol* **28**, 375-430.

Krishnamurthy, K., Heppler, M., Mitra, R., Blancaflor, E., Payton, M., Nelson, R.N. and Verchot-Lubicz, J. (2003). The potato virus X TGBp3 protein associates with the ER network for virus cell-to-cell movement. *Virology* **309,** 135-151.

Liu, J. Z., Blancaflor, E.B. and Nelson, R.S. (2005). The tobacco mosaic virus 126-kilodalton protein, a constituent of the virus replication complex, Alone or within the complex aligns with and traffics along microfilaments. *Plant Physiol* **138,** 1853-1865.

Lough, T. J. a. L., W.J. (2006). Integrative plant pathology: role of phloem long-distance macromolecular trafficking. *Annu Rev Plant Biol* **57,** 203-232.

Lough, T. J., Netzler, N. E., Emerson, S. J., Sutherland, P., Carr, F., Beck, D. L., Lucas, W. J., and Forster, R. L. (2000). Cell-to-cell movement of potexviruses: Evidence for a ribonucleoprotein complex involving the coat protein and first triple gene block protein. *Mol. Plant Microbe Interact* **13**, 962-974.

Lough, T. J., Shash, K., Xoconostle-Cázares, B., Hofstra, K. R., Beck, D. L., Balmori, E., Forster, R. L. S., and Lucas, W. J. (1998). Molecular dissection of the mechanism by which potexvirus triple gene block proteins mediate cell-to-cell transport of infectious RNA. *Mol Plant Microbe Interact* **11**, 801-814.

Lupo, R., Robino, L. and Russo, M. (1994). Immunodetection of the 33K, 98K polymerase proteins in cymbidium ringspot virus-infected and intransgenic plant-tissue extract. *Arch Virol* **138,** 135-142.

Martelli, G. P., Gallitelli, D. and Russo, M. (1998). Tombusviruses. *in* The Plant Viruses. Vol.3 Polyhedral virions with monopartite RNA genomes, R. Koenig, *ed* (New York: Plenum Press), 13-72.

Memelink, J., Vlugt, C.I.M., Linthorst, H.J.M., Derks, A.F.L.M., Asjes, C.J. and Bol, J.F. (1990). Homologies between the genomes of a carlavirus (lily symptomless virus) and a potexvirus (lily virus X) from lily plants. *J Gen Virol* **71**, 917-924.

Mitra, R., Krishnamurthy, K., Blancaflor, E., Payton, M., Nelson, R.S. and Verchot-Lubicz, J. (2003). The potato virus X TGBp2 protein association with the endoplasmic reticulum plays a role in but is not sufficient for viral network for viral cell-to-cell movement. *Virology* **312,** 35-48.

Morozov, S. Y., Lukasheva,L. I., Chernov, B. K., Skryabin, K. G. and Atabekov, J. G. (1987). Nucleotide sequence of the open reading frames adjacent to the coat protein cistron in potato virus X genome. *FEBS Lett* **213**, 438–442.

Morozova, S. Y., Solovyeva, A. G., Kalininaa, N. O., Fedorkina, O. N., Samuilovaa, O. V., Schiemannb, J. and Atabekova, J. G. (1999). Evidence for Two Nonoverlapping Functional Domains in the Potato Virus X 25K Movement Protein *Virology* **260**, 55-63.

Nagata, T., Nemoto, Y. and Hasezawa, S. (1992). Tobacco BY-2 cell line as the "Hela" cell in the cell biology of higher plants. *Int Rev Cytol* **132,** 1–31.

Pillai-Nair, N., Kim, K.H. and Hemenway, C. (2003). Cis-acting regulatory elements in the potato virus X 3' non-translated region differentially affect minus- and plus-strand RNA accumulation. *J Mol Biol* **326,** 701-720.

Pimpl, P., Hanton, S.L., Taylor, J.P., Pinto-DaSilva, L.L., and Denecke, J. (2003). The GTPase ARF1p controls the sequence-specific vacuolar sorting route to the lytic vacuole. *Plant Cell* **15**, 1242–1256.

Pimpl, P., taylor, J.P., Snowden, C., Hillmer, S. Robinson, D.G. and Denecke, J. (2006). Golgi-Mediated Vacuolar Sorting of the Endoplasmic Reticulum Chaperone BiP May Play an Active Role in Quality Control within the Secretory Pathway. *The Plant cell* **18**, 198-211.

Plante, C. A., Kook-Hyung, K., Pillai-Nair, N., Osman, T.A.M., Buck, K.W., Hemenway, C.L. (2000). Soluble, template-dependent extracts from Nicotiana benthamiana plants infected with Potato virus X transcribe both plus- and minus-strand RNA templates. *Virology* **275**, 444-451.

Reichel and Beachy (1998). Tobacco mosaic virus infection induces severe morphological changes of the endoplasmic reticulum. *Proc Natl Acad Sci USA* **95,** 11169-11174.

Restrepo-Hartwig and Ahlquist (1996). Brome mosaic virus helicase- and polymerase-like proteins colocalize on the endoplasmic reticulum at sites of viral RNA synthesis. *J Virol* **70,** 8908-8916.

Ridge, R. W., Uozumi, Y., Plazinski, J., Hurley, U.A. and Williamson, R. E. (1999). Developmental transitions and dynamics of the cortical ER of Arabidopsis cells seen with green fluorescent protein. *Plant Cell Physiol* **40**, 1253-1261.

Ripper, D., Schwarz, H. and Stierhof, Y. (2007). Cryo-section immunolabelling of difficult to preserve specimens: advantages of cryofixation, freeze-substitution and rehydration. *Biol Cell* **10**.

Rubino, L., Russo, M. and Martelli, G.P. (1995). Sequence analysis of the Pothos latent virus genomic RNA. *J Gen Virol* **76,** 2835-2839.

Russo, M., Di Franco, S. And Martelli, G.P. (1983). The fine structure of cymbidium ring spot virus infection in host tissues: 3 Role of peroxisomes in the genesis of multivesicular bodies. *J Ultrastruct Res* **82,** 52-63.

Sambrook, J., Fritsch E.F. and Maniatis, T. (1989). Molecular Cloning: A Laboratory Manual, Ed 2. Cold Spring Harbor Laboratory Press, Cold Spring Harbor, NY.

Samuels, T. D., Ju, H-J, Ye, C.M., Motes, C. M. , Howard, A. R., Blancaflor, E. B., and Verchot-Lubicz, J. (2007). Subcellular targeting and interactions among the Potato virus X TGB proteins. *Virology* **367**, 375-389.

Sanderfoot, A. A., Ahmed, S.U., Marty-Mazars, D., Rapoport, I., Kirchhausen, T., Marty, F., and Raikhel, N.V. (1998). A putative vacuolar cargo receptor partially colocalizes with AtPEP12p on a prevacuolar compartment in Arabidopsis roots. *Proc Natl Acad Sci* **95**, 9920–9925.

Sanderfoot, A. A., Kovaleva, V., Zheng, H., Raikhel, N.V. (1999). The t-SNARE AtVAM3p resides on the prevacuolar compartment in Arabidopsis root cells. *Plant Physiol* **121**, 929-938

Schlegel, A., Giddings, T. H., Ladinsky, M. S., Kirkegaard, K. (1996). Cellular origin and ultrastructure of membranes induced during poliovirus infection. *J Virol* **70**, 6576–6588.

Schwartz, M., Chen, J., Janda, M., Sullivan, M., den Boon, J. and Ahlquist, P. (2002). A positive-strand RNA virus replication complex parallels form and function of Retrovirus capsids. *Mol Cell* **9,** 505-514.

Schwartz, M., Chen, J., Lee, W.M., Janda, M., and Ahlquist, P. (2004). Alternate, virus-induced membrane rearrangements support positive-strand RNA virus genome replication. *Proc Natl Acad Sci USA* **101,** 11263-11268.

Skryabin, K. G., Kraev, A.S., SYu, M., Rozanov, M.N., Chernov,B.K., Lukasheva, L.I. and Atabekov, J.G. (1988). The nucleotide sequence of potato virus X RNA. *Nucleic Acids Res* **16**, 10929–10930.

Sonenberg, N., Shatkin, A. J., Riccardi, R. P., Rubin, M. and Goodman, R. M. (1978). Analysis of the terminal structures of RNA from potato virus X. *Nucleic Acids Res* **5**, 2501-2521.

Sriskanda, V. S., Pruss, G., Ge, X. and Vance, V.B. (1996). An eight-nucleotide sequence in the potato virus X 3' untranslated region is required for both host protein binding and viral multiplication. *J Virol* **70,** 5266–5271.

Suhy, D. A., Thomas, H. Giddings, Jr., and Kirkegaard, K. (2000). Remodeling the endoplasmic reticulum by poliovirus infection and by individual viral proteins: an autophagy-like origin for virus-induced vesicles. *J Virol* **74**, 8953–8965.

Tse. Y.C., M., B., Hillmer, S., Zhao, M., Lo, S.W., Robinson, D.G. and Jiang, L. (2004). Identification of multivesicular bodies as prevacuolar compartments in Nicotiana tabacum BY-2 Cells. *Plant cell* **16**, 672-693.

Verchot, J., Angell, S.M. and Baulcombe, D.C. (1998). In vivo translation of the triple gene block of Potato virus X requires two sub genomic mRNAs. *J Virol* **72,** 8316-8320.

Watanabe, T., Honda, A., Iwata, A., Ueda, S., Hibi, T. and Ishihama, A. (1999). Isolation from tobacco mosaic virus-infected tobacco of a solubilized template-specific RNA-dependent RNA polymerase containing a 126K/183K protein heterodimer. *J Virol* **73,** 2633–2640.

Wessel, D. a., U. I. (1984). A method for the quantitative recovery of protein in dilute solution in the presence of detergents and lipids *Anal Biochem* **138**, 141-143.

White, K. A., Bancroft, J.B. and Mackie, G.A. (1992). Mutagenesis of a hexanucleotide sequence conserved in potexvirus RNAs. *Virology* **189,** 817-820.

VITA

DEVINKA C N BAMUNUSINGHE

Candidate for the Degree of

Master of Science

Thesis: DETERMINATION OF SUB-CELLULAR LOCALIZATION OF POTATO VIRUS X REPLICASE DURING INFECTION

Major Field: Plant Pathology

Biographical:

Personal Data: Born in Sri Lanka on July 2nd to Chandrasiri and Sita Bamunusinghe and migrated to USA in 2005.

Education: Received Bachelor of Science (Special) degree, Majored in Botany, Microbiology and Molecular Biology from University of Ruhuna, Sri Lanka. Completed the requirements for the Master of Science in Plant Pathology at Oklahoma State University, Stillwater, Oklahoma in May, 2008.

Experience: Graduate Research Assistant, Department of Entomology and Plant Pathology, Oklahoma State University, Stillwater, OK, August 2005 to May 2008
Technician (Volunteer), Laser capture micro-dissection lab, Fox Chase Cancer Centre, Philadelphia, 2005
Assistant Lecturer (2004 to 2005), Teaching Assistant (2002-2004), Undergraduate Research assistant (2001 to 2002) Department of Botany, University of Ruhuna, Sri Lanka.

Professional Memberships:
Member, American Society for Virology (ASV) 2006 -2007
Member, Oklahoma Microscopy society (OMS) 2007

Name: DEVINKA C N BAMUNUSINGHE Date of Degree: May, 2008

Institution: Oklahoma State University Location: Stillwater, Oklahoma

Title of Study: DETERMINATION OF SUB-CELLULAR LOCALIZATION OF POTATO VIRUS X REPLICASE DURING INFECTION

Pages in Study: 79 Candidate for the Degree of Master of Science

Major Field: Plant Pathology

Abstract:

Potato virus X (PVX) encodes a 166 kDa replicase. RNA virus replication typically occurs along cellular membranes. Since recent studies showed that PVX TGBp2 and TGBp3 proteins associate with endoplasmic reticulum(ER), experiments were conducted to find out whether PVX replicase is also ER associated. Protoplasts and plants were inoculated with PVX.GFP-TGBp2 and PVX.TGBp3-GFP. Following immunolabeling and confocal or electron microscopy, the PVX replicase, TGBp2, and TGBp3 were seen in vesicles and along the ER. Furthermore replicase, BiP (ER resident protein) and GFP labelling were mainly observed in ER and ER-derived vesicles. The ER-derived vesicles were novel virus-induced structures containing virions. Sucrose gradient fractionation, immunoblot analysis, and densitometry were conducted to determine if the PVX replicase, TGBp3-GFP and BiP co-fractionate with other components of the endomembrane network. PVX replicase, TGBp3-GFP, and BiP were found in the ER-containing fraction, providing further support that these PVX proteins target to the ER or ER-derived vesicles.

ADVISER'S APPROVAL: Dr. Jeanmarie Verchot–Lubicz